CANADA

DEPARTMENT OF
ENERGY, MINES AND RESOURCES
MINES BRANCH
OTTAWA

ELEVATED-TEMPERATURE PEELING FAILURE OF GALVANIZED COATINGS

J. J. SEBISTY AND D. PAPENFUSS

PHYSICAL METALLURGY DIVISION

OCTOBER, 1971

REVISED

Research Report R 245

Price $1.00

Available by mail from Information Canada, Ottawa,
and at the following Information Canada bookshops:

HALIFAX
1735 Barrington Street

MONTREAL
1182 St. Catherine Street West

OTTAWA
171 Slater Street

TORONTO
221 Yonge Street

WINNIPEG
393 Portage Avenue

VANCOUVER
657 Granville Street

or through your bookseller

Price: $1.00 Catalogue No. M38-1/245

Price subject to change without notice

Information Canada
Ottawa, 1972

Mines Branch Research Report R 245

ELEVATED-TEMPERATURE PEELING FAILURE OF GALVANIZED COATINGS

by

J. J. Sebisty* and D. Papenfuss**

- - -

ABSTRACT

The elevated-temperature peeling failure of conventional galvanized coatings was investigated with the object of defining the factors which influence and control the process.

Two different heating deterioration modes revealed were found to be dependent on the chemical composition of the coating. Above a critical limit of 0.001% Pb, the outer zinc layer separated in the characteristic manner, and similar failure was induced by alloying with bismuth, indium, thallium, and tin. Below this lead limit, and with additions of aluminum, cadmium, magnesium, nickel, silver, vanadium, and zirconium, the coating remained completely intact and the outer zinc layer gradually disappeared by diffusion dissolution. The rate of both reaction modes was primarily influenced by the time and temperature of heating and the coating thickness.

Mechanisms which attempt to account for the peeling process are reviewed and an alternative explanation is offered which is more nearly consistent with the observed facts.

Practical implications of the results are discussed, inclusive of transformation effects in the iron-zinc alloy layers which relate to the kinetics of the galvanizing reaction.

---

* Research Scientist, Non-Ferrous Metals Section, Physical Metallurgy Division, Mines Branch, Department of Energy, Mines and Resources, Ottawa, Canada.

** Formerly Research Metallurgist, Canadian Zinc and Lead Research Committee.

Direction des mines

Rapport de recherches R 245

La Desquamation à haute température des revêtements galvanisés

par

J.J. Sebisty* et D. Papenfuss**

Résumé

On a fait des recherches approfondies sur la desquamation à haute température des revêtements galvanisés conventionnels ayant pour but de définir les facteurs qui influencent et contrôlent le procédé.

On a trouvé que deux modes différents de détérioration à la chaleur dépendaient de la composition chimique du revêtement. Quand la teneur en plomb dépasse la limite critique de 0.001% la couche extérieure de zinc se sépare de façon caractéristique, et un phénomène semblable se produit quand on y allie du bismuth, de l'indium, du thallium et de l'étain. Quand la teneur en plomb ne dépasse pas cette limite le revêtement reste complètement intact et la couche extérieure de zinc disparaît graduellement par diffusion avec l'addition de l'aluminium, du cadmium, du magnésium, du nickel, de l'argent, du vanadium, et du zirconium. La vitesse de réaction des deux modes a été influencée essentiellement par le temps et la température du chauffage et l'épaisseur du revêtement.

On passe en revue aussi les différents mécanismes utilisés pour essayer d'expliquer le procédé de desquamation et on offre une explication alternative qui est plus logique si on se base sur les faits observés.

Enfin on discute les implications pratiques des résultats, incluant les effets de transformation sur les couches d'alliage fer-zinc ayant rapport à la cinétique de la réaction de galvanisation.

---

*Chercheur scientifique, Section des métaux non ferreux, Division de la Métallurgie physique, Direction des mines, ministère de l'Energie, des Mines et des Ressources, Ottawa, Canada.

**Autrefois chercheur métallurgiste, Comité canadien de recherches sur le zinc et le plomb.

CONTENTS

TABLES

FIGURES

(Figures, concluded) Page

- - - - -

INTRODUCTION

A service performance limitation of conventional galvanized coatings at elevated temperatures is a tendency of the outer zinc layer to peel or spall. This response is related to the coating microstructure which is composed of reaction phases of iron-zinc alloys in layer formation (ζ, δ_1 and Γ in that order beneath the zinc). On heating to moderately elevated temperatures, or under certain conditions of cooling after galvanizing, the adherence of the outer zinc layer is destroyed. Some degree of mechanical keying may retain the layer in place, but more usually it peels away. Loss of grain boundary cohesion can also occur, causing the zinc layer to spall as individual zinc grains. Unlike the flaking behaviour during bending or impact deformation, which can involve separation of the entire coating, the underlying iron-zinc alloy layers are relatively unaffected in the process; they remain attached to each other and to the steel base.

Although this phenomenon is well known, there is little published evidence of any systematic study of its nature and cause and of the factors which influence and control the peeling mechanism. Such study was the basis for the present investigation, and was further prompted by prior work on continuous strip [1-3] and on thick-wall tubing, angle, and bar products [4]. The investigation was principally an examination of the behaviour of a wide range of experimental sheet coatings of conventional composition or otherwise alloyed. These all conformed to the basic microstructure of coatings obtained in general galvanizing practice. A commercial sheet product fitting this description was also examined. The investigation was performed with the co-operation and support of the Canadian Zinc and Lead Research Committee and of the International Lead Zinc Research Organization, Inc.

PRIOR WORK

The study on thick-walled products [4] confirmed the prior observation of Hershman et al [5] that the zinc peeling mechanism depends on both time and temperature of heating. It was further established that microstructural characteristics of the coating and, in particular, the coating thickness (length of the diffusion path) influenced the rate of deterioration of the Zn-ζ bond. Hershman concluded that peeling was due to the Kirkendall effect and was associated with cavity formation by condensation of lattice vacancies at the Zn-ζ interface. This explanation appears oversimplified and does not, for example, explain the behaviour of lead-free coatings found in the present investigation. The latter was briefly reported in a discussion [6] on Hershman's work and is described in more detail later in this paper. Hughes [7] also speculated that peeling either after galvanizing or on heating to just below the melting point of zinc may be associated with the behaviour of lead. No further explanation was given.

Other reports and scattered notes to be found deal with peeling failure occurring after galvanizing. Most frequent reference is to the detrimental influence of slow cooling that may arise from piling or nesting coated products while still hot after withdrawal from the bath [8]. Typical failures related to such practice have been reported for culvert stock [9] and tubing [10]. It was also found [11] that with some types of cold-reduced and annealed material, any interruption in the cooling rate caused the free zinc to separate. This was avoided if cooling through the critical temperature region around 390°C (735°F) was fast enough. Because of the apparent connection with the processing of the steel base, it was suggested that the surface layer of the steel was in some way involved.

A similar conclusion was reached [12] to explain peeling at the edges and centre on one side of sheet that was not stacked. Cooling effects were discounted and variations in the steel surface produced by annealing were thought to be primarily responsible. From sporadic occurrences of peeling on both sides of sheets and from failure to initiate zinc-layer separation by deliberate hot stacking, Haarmann [13] inferred that some other factor besides the influence of heating must contribute to the observed poor adhesion of the zinc layer.

Bablik and co-workers [14] insisted that peeling was due mainly to the threefold difference in coefficient of expansion between zinc and iron (39.7 and 11.7 μ in./in./°C, respectively). They cautioned against slow cooling, as well as very drastic cooling to reduce alloying, because either extreme might cause separation owing to the higher contraction rate of zinc. Teindl et al [15] offered the same explanation, again without any supporting evidence.

Reference to the influence of the environment in an elevated-temperature application has also been made [16]. Minimum details were given beyond the fact that peeling of conventional galvanized coatings on sterilizer racks was less prevalent in steam heated than in electrically heated apparatus operated at 275°C (525°F).

Of some relevance to this investigation are elevated-temperature peeling studies made on aluminized coatings. The explanation by Tagaya et al [17] corresponds to that proposed by Hershman [5] for galvanized coatings, namely, that voids are formed by lattice vacancies collecting at the aluminum and aluminum-iron interface. A further qualification was that spalling was due to the voids acting in conjunction with shearing stresses induced by the difference in thermal expansion of aluminum and the underlying alloy layer. Saga [18] examined the effect of the heating rate on the peeling of the aluminum layer and found that separation was restricted to rates lower than 4°C/min (7°F/min). Above 15°C/min (27°F/min), the aluminum layer was uniformly diffused into the alloy layers and there was no evidence of peeling.

EXPERIMENTAL PROCEDURE

The investigation was principally on laboratory-prepared coatings made in iron-saturated (0.03% Fe) special high-grade (99.99%) zinc baths, with and without lead and other additions (Table 1). Apart from several lead levels examined, a single, relatively large addition of each of the other elements, aluminum, bismuth, cadmium, indium, nickel, silver, thallium, tin, vanadium, and zirconium, was tried.

The steel was rimming-grade 24-gauge (0.025-in. or 0.6-mm) sheet. The bath temperature was 450°C (840°F) in all cases and immersion times were 1, 4, 10, and 20 minutes. Other details on the galvanizing procedure may be found elsewhere [19].

The principal series of tests involved the heating of panels 2 in. x 2 in. (5 x 5 cm) in a forced-air convection furnace at one or more of the following temperatures: 275°C (525°F), 300°C (570°F) or 400°C (750°F). The panels were racked vertically and heating periods varied from 5 minutes to 2 weeks. All samples were air-cooled. Miscellaneous tests were made on samples heated in evacuated capsules, in a silicone oil bath, and after galvanizing at a high temperature or by double dipping. Also examined was the effect of heating a few degrees above and below the Zn-Pb eutectic temperature of 318°C (605°F), as well as the behaviour of commercial sheet coated by the conventional sheet-galvanizing process. The coatings were evaluated before and after heating by surface inspection (macro and micro), metallographic examination of cross sections, coating stripping tests, and by electron probe microanalysis, X-ray diffraction, and microhardness tests. Etchants developed by Rowland [20] were used to reproduce metallographic effects.

OBSERVATIONS AND RESULTS

To facilitate discussion, the terms "leaded" and "lead-free" are used with reference to the coatings galvanized in iron-saturated baths with and without lead, respectively. Those prepared with the other alloying additions, whether leaded or lead-free, are described as "alloyed" coatings. Coating evaluation tests are summarized in Table I, and metallographic effects are illustrated in Figures 1 to 20.

Leaded Coatings

Coatings made in iron-saturated zinc baths containing 1.0% Pb usually had a bright surface finish. Polygonal spangle grains about 0.5 in. (12 mm) in diameter were evident with immersion times up to 4 minutes. Somewhat larger and more irregularly shaped grains were formed at longer immersion times of 10 and 20 minutes, and slight depression of the grain boundaries was also apparent.

(a) Pitting of Zinc Layer

An initial effect of heating at 275°C (525°F) with the leaded coatings galvanized for 1 and 4 minutes was the formation of pits on the surface. These increased in number, size, and depth of penetration with increasing exposure time. Significantly, an increase in coating thickness decreased the rate of pit nucleation and growth. With continued enlargement and coalescence of the pits, the stage was reached where, locally, no zinc remained and the underlying iron-zinc alloy was exposed.

As illustrated in Figure 1, the pits in many grains showed well-defined orientation faceting. One or more facet edge was always directionally aligned in any one grain, and a principal edge usually ran parallel to slip banding on the surface. Closely packed lines of pits as in Figure 1(a) appeared to be associated with scratches or sub-boundaries. The large dark patches in Figure 1(b) represent local depletion of zinc where the pits had merged. Within some grains, the pits took the form of shallow, irregular, or hexagonal-shaped stepped depressions, scattered in random distribution and with no evident orientation. Examples can be seen on the left side of Figure 1(a). Slip banding was not evident on these grains which were apparently oriented with the basal plane more nearly parallel to the coating surface. These depressions also eventually blanketed the grains so affected but thinning of the zinc layer was relatively uniform rather than localized, and the open structure associated with faceted pitting was not developed.

The same pitting features were reproduced on all the leaded coatings heated at 300°C (570°F) and 400°C (750°F). As before, the rate of pit nucleation and growth and of zinc depletion progressively increased with temperature. The effect of coating thickness was also more clearly revealed; for equivalent exposure conditions, fewer pits formed and the growth rate was significantly reduced as the coating thickness increased. As also to be expected because of the thicker outer-zinc layer, the eventual pit size attained was larger with thicker coatings as shown in Figure 1(c).

In cross section, the faceted surface pits generally took the form of triangular or polygonal indentations. The depth of penetration increased with exposure time and, in advanced stages, represented a significant proportion of the thickness of the outer zinc layer. Typical examples formed at 275°C (525°F) are shown in Figure 4. It is to be noted that subsequent, gradual disappearance of the zinc was not due solely to enlargement of the surface pits. During, or after, separation of the layer, which is described in the next section, well-defined angular indentations were also developed on the under surface. This accounts for the angular disconnected particles constituting the apparent remains of the zinc layer after extended heating, as in Figure 4(e) and (f). The layer at these stages was still a continuous but heavily pitted film. Other examples of the undercutting effect can be seen in

Figures 5 and 6. Of interest is its different form at higher temperatures and, particularly, with very thick coatings (20-minute immersion) as in Figure 7(c). As shown --- the underside indentations frequently assumed large rounded shapes, and the volume of zinc removed therefrom was much greater than from pitting of the surface.

With pure bulk materials, the usual explanation for surface pits of the type observed is that they represent dislocation imperfections where segregation of impurity atoms and precipitation of lattice-vacancy defects occur. On chemical etching after thermal treatment, geometrical-shape pits form either because of preferential attack at such impurity sites or because the region where the dislocation meets the surface is more highly strained. Typical etch-figure distributions found with high-purity zinc doped with small tin additions are described by Bassi et al [21].

There is evidence that the same structures can be developed by "thermal etching". For example, Rais et al [22] observed hexagonal pits after vacuum annealing of zinc monocrystals and related these to high-energy active sites on the surface. According to Kamel [23], room temperature ageing for several days was apparently sufficient to cause spirally terraced rectangular pitting on basal-plane cleavage surfaces of zinc single crystals. Migration of lattice vacancies to the surface along dislocations was suggested as being responsible for pit nucleation. Subsequent accelerated enlargement of the pits was thought to be related to surface diffusion and unspecified corrosion factors. Doherty et al [24] also attributed oriented pitting on electropolished aluminum single crystals to condensation of vacancies. The pits were formed during cooling from an elevated temperature and not during heating or while a specimen was held at a constant temperature.

Detailed study of the origin of pitting in the present work was beyond the scope of the investigation because of the many samples treated. Also, insofar as correlation with lattice-defect phenomena was concerned, unavoidable limitations were imposed by the macroscopically rough surface and, presumably,by the stressed state of the as-cast outer zinc layer. However, it was established that the rates of nucleation and growth of the pits and of subsequent dissolution of the zinc layer were dependent on the time-temperature heating conditions and on the coating thickness. The observed effects therefore suggest that the mechanism involved diffusion of zinc atoms to the Zn-ζ interface and an outward migration of vacancies to the surface pits.

A connection between surface pitting and the iron-zinc diffusion reaction was further provided from prior tests with continuous strip coatings [1,2]. In this case, heating normally produces nodules of iron-zinc alloy as the first major stage in deterioration. These were frequently observed to be surrounded by a ring of faceted pits as in Figure 3(a). The cross section in Figure 3(b)

shows a typical alloy nodule with faceted indentations on the adjacent zinc surface as well as on the underside of the separated layer. In the case of the surface nucleated pits, movement of zinc atoms to feed the growth and of lattice vacancies to the surface appears to be the mechanism of formation. Less certain is the origin of faceted indenting on the lower side of the zinc layer. If this represents initiation of the zinc separation process, then vacancy movement to the Zn-ζ interface according to the Kirkendall effect, as discussed later, must be involved. On the other hand, if the undercutting is simply indicative of secondary zinc dissolution from Kirkendall voids by surface diffusion, vapor transport, oxidation corrosion, or some other mechanism, it is not directly relevant to the primary peeling reaction.

(b) Separation of the Zinc Layer

Apart from the pitting effects already described, Figure 4 shows other features of the zinc layer separation process which occur on heating of conventional galvanized coatings. The series shown is of 1-minute leaded coatings heated at 275°C (525°F).

The initial microstructural evidence of separation after 5 hours was etch-darkening along the Zn-ζ interface, as shown in Figure 4(b). At 12 hours, dissolution of the matrix zinc between the outermost crystals of the ζ layer was observed as in Figure 4(c) and the more or less continuous gap formed effectively destroyed the Zn-ζ bond. The zinc layer could be easily peeled away with adhesive tape to expose a black oxidized finish yielding a powdery residue on rubbing. This stage corresponds to the reaction failure time given in Table I. The peeled layer had the appearance of fine lacework and readily broke up into individual grains because of complete loss of cohesion at the grain boundaries. An exaggerated form of such break-up in an alloyed coating heated at a higher temperature is illustrated in Figure 2. This is more representative of an in-plant type of failure where the separated zinc pulls away completely. Such "popping" was not observed with the experimental coatings and, although separated, the zinc layer retained some mechanical keying and remained in place unless deliberately chipped or peeled away.

More prolonged heating effects shown in Figures 4(e) and (f) indicate gradual disappearance of the detached zinc layer. Although extensive fragmentation is apparent, the layer in situ was still a continuous film but showed the characteristic lack of cohesion at the grain boundaries when peeled away. The gap width also increased as shown and was probably related, in part, to tearing out during metallographic polishing of undermined ζ crystals and particles of zinc.

Other transformation effects, occurring in the underlying iron-zinc alloy layers during and after separation, are worthy of comment. Of particular note is that, for the range of heating times covered in Figure 4, the bonding remained intact at the ζ - δ_1, δ_1 - Γ, and Γ - steel interfaces.

It can also be seen that the ζ phase showed most rapid growth in the early stages of heating. However, before the separation end-point was reached, the growth rate of the δ_1 phase increased and was accompanied by well-defined partial re-solution of the thin Γ phase. This latter effect coincided with the formation of dark-etching needle crystals in the δ_1 layer, shown more clearly in Figure 4(e). Electron probe microanalysis (25) confirmed these to be high-iron "coherent" δ_1. Figures 4(e) and (d) also indicate that growth of the Γ phase was later restored, giving a uniform and increasingly thick band adjacent to the steel surface. In these advanced stages, the reciprocity in growth of the phases was again evident in that rapid Γ growth coincided with reduced thickness in the δ_1 layer.

Figure 5 shows that the peeling and microstructural effects described above were duplicated in the 4-minute coatings heated at 275°C (525°F). With the longer diffusion path, however, the various deterioration stages were slowed down. For equivalent exposure times, pitting of the outer zinc layer was less pronounced as mentioned earlier. Etch-darkening at the Zn-ζ interface was not apparent until 8 hours and well-defined cavities formed at around 12 hours as in Figure 5(b). More notably, up to 24 hours heating was required before the layer could be peeled away (Table I). The subsequent rates of zinc dissolution and fragmentation and of iron-zinc alloy transformation changes were also retarded. Nucleation and growth of the "coherent" δ_1 needles at the expense of the Γ phase is again evident in Figures 5(c) and (d).

The influence of coating thickness was more clearly defined in the higher-temperature tests. Estimated times for separation of the zinc layer (Table I) show that Zn-ζ bond failure with the 1-minute coatings was complete after 4 hours at 300°C (570°F), and after only 5 minutes at 400°C (750°F). The same stage required 24 hours and 2 hours at these respective temperatures with the much thicker 20-minute coatings. This characteristic dependence of time to failure on coating thickness is highlighted by the relative degrees of damage in Figures 6 and 7(b). It will be noted that the 20-minute coating in Figure 7(b) was heated twice as long as the thinner coatings in Figure 6. On a similar time basis, therefore, its resistance to deterioration would have been still better than shown.

The coating microstructures in Figures 6 and 7 are of interest for other reasons. In particular, Figures 6(b), 7(b), and (c) provide more conclusive proof that separation of the zinc layer is initiated by reaction dissolution of the matrix zinc surrounding the fringe crystals of the ζ layer. The disappearance of intergranular particles of zinc contained well down in the columnar ζ further indicates that the reaction is not confined to a band along the Zn-ζ boundary as is the case with thin coatings. The marked fissuring disintegration of the ζ phase and the well-defined evidence of a duplex-Γ structure in Figure 7(d) are also of interest. Significantly, the secondary layer next to the steel base appears in a more uniform and

continuous form with the shorter heat treatment in Figure 7(c). This is discussed in a following section.

Attention is drawn to the practical implication of the inter-dependence between the coating thickness and the time to separation defined for the leaded coatings in Table I. This relates specifically to the in-plant type of zinc layer separation that may occur because of slow cooling after withdrawal from the bath. It is evident that only relatively thin coatings (< 2 oz/sq ft - 610 g/m^2) should be susceptible to peeling on retarded cooling through the critical temperature region around 400°C (750°F). Even in this case, the cooling rate would have to be equivalent in its effect to a 5-minute hold at this temperature. For thicker coatings (> 2.5 oz/sq ft - 715 g/m^2) any delay in cooling would have to be equal to about a 30-minute hold, and considerably longer for very thick coatings. Reproducing this equivalent-delay condition in practice would be highly unlikely if reasonable precautions were taken to ensure adequate cooling after withdrawal.

Lead-Free Coatings

As already noted, the designation "lead-free" refers to coatings prepared in baths of iron-saturated special high-grade (99.99%) zinc. The lead content was 0.001% or less. With all immersion times (1 to 20 minutes), the coatings had a bright metallic finish with very small grains averaging less than 0.05 in. (1 mm) in diameter. Compared with the leaded coatings, this represents a grain size reduction of about 10 times.

A detailed comparison of the thermal pitting behaviour of lead-free and leaded coatings was not made. In general, however, it appeared that for comparable thicknesses and heating conditions, the number and size of pits were always less in the lead-free coatings. Figure 8(a) illustrates the grain-oriented pits and stepped depressions found on the 1-minute coatings after 5 hours heating at 275°C (525°F). After 12 hours, large dark patches as in Figure 8(b) were evident and, within 1 day, the outer zinc layer had completely disappeared, exposing the oxidized surface of the underlying ζ phase. Of most significance was the observation that at no stage in this process was there any separation of the zinc layer. It could neither be chipped nor peeled away and remained firmly adherent even after being reduced to a thin layer. This reaction mode in Table I is defined as "zinc layer diffused".

The same behaviour was noted with the 4-minute lead-free coatings at 275°C (525°F) except, as before, fewer pits were nucleated and 2 days was required for complete disappearance of the zinc layer. Estimated times for the same effect at 300°C (570°F) and 400°C (750°F) for a range of coating thicknesses are also given in Table I. As expected, the "zinc-diffused" end-point was reached more quickly with increasing temperature and progressively more slowly with increased coating thickness. Thus,

the dependence of the zinc dissolution mechanism on the diffusion path length was again demonstrated. None of the tests showed evidence at any stage of loosening of the zinc layer and it could not be dislodged even by vigorous scraping.

Typical metallographic effects observed with the 1- and 4-minute coatings at 275°C (525°F) are shown in Figures 9 and 10. Both series provide positive evidence of the different reaction mode of the lead-free coatings. Rapid and continuing transformation of the outer zinc layer to iron-zinc alloy was always reflected in total absence of any bonding deterioration at the Zn-ζ interface. On all flat sheet sections examined, cavity formation at the interface was practically non-existent except for randomly scattered holes as in Figures 9(d) and 10(c). These developed in advanced stages of the zinc thinning process and, being isolated localized defects, they had no detrimental effect on the bonding of the surrounding zinc. As discussed later, special instances of cavity development were observed in the open fan-like iron-zinc alloy structure at corners and, to a lesser extent, on small-radius convex surfaces.

Comparison of the respective coatings in Figures 9 and 10 with those in Figures 4 and 5 reveals various effects related to the uninterrupted zinc diffusion in the lead-free coatings. A thicker ζ layer was developed during the shorter heating periods and was followed by accelerated growth of δ_1 (inclusive of the high-iron "coherent" needles) at the expense of Γ. An apparent anomaly was indicated at the longest exposure of 8 days. In the respective photomicrographs, more pronounced growth in the δ_1 and Γ layers is shown by the leaded coatings in Figures 4(f) and 5(e). This was a real effect and was presumably related to the lesser total depth of iron-zinc alloy because of the restriction on inward movement of zinc after separation. More rapid growth of the higher-iron phases would thereby be expected in advanced reaction stages.

These various metallographic features were more strikingly reproduced in the thicker range of coatings tested at 300°C (570°F) and 400°C (750°F). The 20-minute coating series in Figure 11 provide the best examples. Most prominent is the complete absence of any evidence of Zn-ζ interface separation. The islands of zinc dispersed intergranularly well-down in the ζ layer are also intact. Comparison of Figure 11(c) with 7(c) highlights the pronounced δ_1 growth in the lead-free case. Almost total dissolution of the ζ phase has occurred and only small pockets remain at the surface. This confirms that by retention of bonding at the interface, the continuous supply of zinc thereby maintained was effective in sustaining a higher reaction rate. As expected, the exposed δ_1 surface was hard and abrasion resistant and had a characteristic dark-grey finish.

Equally striking in Figure 11(d) is the almost total absence of fissuring which contrasts with the pronounced break-up of the exposed ζ phase in the leaded coating of Figure 7(d). The enhanced resistance to deterioration of the δ_1 phase was thus clearly demonstrated. The duplex-Γ structure can also be seen with the layer adjacent to the steel surface again being more uniform and continuous at the shorter heating time in Figure 11(c). The leaded coatings in Figure 7 showed the same sacrificial re-solution with increased heating time. This was also characteristic of the Γ phase as discussed previously and illustrated in Figures 4 and 5 and in 9 and 10.

Critical Lead Limit

To establish the minimum lead content which would cause separation of the outer zinc layer, coatings were prepared with different amounts of pure lead (99.99%) added to iron-saturated special high-grade (99.99%) zinc. The latter contained <0.001% Pb as previously noted. The additions were varied in several steps over the range 0.0015 to 1.0% as indicated in Table I. Samples were galvanized for 1 and 4 minutes at 450°C (840°F) and subsequently heated at 300°C (570°F). Coating weights are listed in Table I, and some typical surface and metallographic effects are illustrated in Figures 12 and 13.

Most significant was the observation that all coatings with 0.0015% or more lead showed the characteristic formation of a continuous gap at the Zn-ζ interface. Figure 13 illustrates the contrasting behaviour at this critical lead limit and below it. As before, the onset of separation was a direct function of coating thickness, i.e., the diffusion path length. Although systematic tests were not made, there were indications that increasing the lead content initiated gap formation more rapidly. More positive evidence of this has been reported (26) from tests with low-lead and lead-saturated coatings heated at and above 350°C (660°F).

It is to be noted that lead also produces marked grain coarsening in the outer layer (Figure 12). Thus, the more rapid failure rate with high-lead coarse-grained coatings, having less grain boundary area, discounts grain boundary diffusion as a dominant factor in the separation process. The irrelevance of zinc grain size was further demonstrated by the separation failure of the coatings with only 0.0015% Pb even though the grain size was as fine as in the lead-free coatings. At the same time, the inherently higher diffusion rate at grain boundaries may have contributed to the sustained and higher reaction rate with the fine-grained lead-free coatings. It is unknown whether this is cause or effect, or is otherwise immaterial with respect to the retention of Zn-ζ bonding.

A further point of practical interest was that as long as the separated layer in the leaded coatings was neither disturbed nor lifted out of place,

it eventually disappeared by continued reaction. Adherence of the layer by mechanical keying was nevertheless minimal as indicated by the dark corner patches in Figures 12(b) to (d). These represent areas where the zinc was readily peeled off with adhesive tape. Since the layer otherwise remained keyed in place, it might be inferred that its protective usefulness as part of the coating was retained to some degree. However, any practical exploitation thereof, in the hope that the layer would not become detached, would be unwise. Weakening of the zinc layer as a structural entity was further shown by the coincidence of tearing with the zinc grain boundaries in Figure 12(d). A more exaggerated case of loss of grain boundary cohesion can be seen in Figure 2.

The contrasting behaviour of the lead-free coatings (<0.001% Pb) at 300°C (570°F) and the other temperatures tried has already been discussed in the previous section. By way of emphasis, this group exhibited gradual disappearance of the zinc layer under all conditions without any evidence of bond failure at the Zn-ζ interface. The typical grey appearance of the exposed ζ surface is illustrated in Figure 12(a). An earlier heating stage in the coating microstructure of Figure 13(a) again reveals the freedom from interface failure, although appreciable zinc remains. Local emergence of ζ where the covering zinc has reacted completely can also be seen.

Attention is drawn to special cases of interface cavity development at corners or on curved surfaces with coatings containing <0.001% Pb. Figure 14(a) is typical and shows fine intergranular voids in the open fan-like ζ structure at a corner. The normal structure adjacent to the corner is expectedly free of any interface deterioration. In contrast, Figure 14(b) shows the gross cavitation at a corner, merging into distinct separation of the zinc layer away from this area, when 0.0015% Pb was present. A larger radius of curvature, as with 1-in. diameter tubing, was also found to be somewhat susceptible to cavity formation. This was revealed in heating tests after regalvanizing of commercial tubing in special high-grade zinc. From these results, it appears that the role of lead can be influenced by the morphology of the ζ phase.

A not uncommon explanation for the effect of lead is that it accumulates at the Zn-ζ boundary and acts as a barrier to the counter-current diffusion movement of zinc and iron. Such segregation on a macro scale appears unlikely because lead is present in the zinc layer as randomly scattered globules. Electron probe microanalysis has confirmed such a distribution [25, 26]. Furthermore, the solid solubility of lead in zinc is very low (<0.0002%). Thus, the small volume of zinc that could diffuse inward before the interface gap forms would not be expected to leave a uniformly distributed and continuous layer of lead at the interface.

The concentration of lead in this region was examined by X-ray diffraction with iron-filtered cobalt radiation. The samples were powdery residues scraped from the exposed ζ surface of leaded coatings. Very complex patterns were obtained, and attempts to identify either iron- or lead-containing constituents were unsuccessful. More positive results claimed from electron probe analysis (26) disproved the existence of an interfacial lead film. Moreover, there was no obvious association between interface cavities and identifiable lead particles present.

Radioactive Tracer Tests

It is known that thallium reacts like lead when alloyed with zinc. Advantage was taken of this behaviour in an attempt to get further information on the role of lead by application of radioactive tracer techniques. A 1.0% addition of Tl^{204} was made to a special high-grade zinc bath and samples were galvanized from 1 to 20 minutes at 450°C (840°F). The coatings had a poor surface appearance because of drag-out of oxidation products but were otherwise acceptable. They were heated at 300°C (570°F) in an argon atmosphere and subsequently taper-sectioned and polished for application of Contrast Process Ortho film for up to 48 hours. Of principal interest was the distribution of thallium in the zinc layer, at the Zn-ζ interface, and within the iron-zinc alloy layers.

Apart from separation of the zinc layer as occurred with lead, the experiments met with only limited success because of the small magnifications possible (up to 10x). It was nevertheless indicated that the iron-zinc phases were apparently thallium-free. By inference, therefore, lead could not be considered to have a direct influence on formation of the intermetallic alloy layers. The tests were otherwise inconclusive and failed to reveal evidence of thallium segregation in the outer zinc layer or at the Zn-ζ interface.

Commercial Sheet

Heating tests were made with 24-gauge commercial sheet coated by the conventional sheet-galvanizing process. It had typically large spangles as to be expected from the coating process and the composition of 0.44% Pb, 0.26% Sn, and 3.28% Fe. The coating thickness was 2.0 oz/sq ft and the microstructure, Figure 15(a), shows a normal layer formation of iron-zinc alloys. A chromating treatment had apparently been applied after galvanizing.

In all respects, the coating behaved like the leaded experimental coatings of similar thickness. Zinc layer separation was complete after 4 hours at 300°C (570°F) and after 5 minutes at 400°C (750°F). The latter failure, along with typical microstructural changes after longer exposures, can be seen in Figure 15. Within 40 minutes, for example, there was almost total conversion of ζ to δ_1, as evident in Figure 15(c). At the later stage in Figure 15(d), significant Γ growth is apparent. With the more prolonged

heating represented in Figure 15(e), the duplex-Γ structure formed the major part of the coating that remained. It is also evident that the dark-etching secondary layer between the Γ and the steel base is responsible for the characteristic intergranular penetration and undermining of grains in the steel.

Other Tests

Exploratory tests on leaded and lead-free experimental coatings were made by heating samples for up to 20 hours at a few degrees above and below the Zn-Pb eutectic temperature of 318°C (605°F). The respective coatings reproduced the same effects as already described. Melting of the lead constituent as a factor in zinc layer separation was, therefore, further discounted. In a similar manner, the peeling of leaded coatings was unaltered by heating in evacuated capsules or in a silicone oil bath. Thus, the possibility of oxygen diffusion through the zinc layer to form the interface gap by an oxidation mechanism can also be ignored.

It is of interest that panels initially galvanized in a lead-free bath and then redipped in a lead-containing bath were equally susceptible to separation of the zinc layer . The reverse procedure, i.e., starting with a leaded commercial coating on tubing, stripping and regalvanizing in a lead-free bath, effectively prevented peeling of the zinc. Some interface cavities were formed but, as discussed earlier, these were related to the surface geometry of the tubing.

In another series, leaded and lead-free samples were galvanized at 510°C (950°F). At this temperature, the ζ phase cannot form and the zinc is in direct contact with δ_1 . In conformity with all other heating tests, the leaded coatings again showed separation in the characteristic manner, whereas interface bonding was unaffected with the lead-free coatings. The separation mechanism was thus indicated to be independent of the iron-zinc phase in contact with the zinc layer.

Alloyed Coatings

For further investigation of the peeling mechanism, heating tests were tried with leaded and lead-free experimental coatings alloyed with other additions (Table I). Aluminum and tin were selected because of their common occurrence in commercial coatings, whereas magnesium, nickel, silver, vanadium, and zirconium were of interest because of their effects on coating formation [19]. Bismuth, cadmium, indium and thallium were included because of their low melting points or other similarities to lead. For this group and for tin, an arbitrary addition of 1.0% was used. With all others, the amount added generally corresponded to the established level of maximum effectiveness.

It is of note that bismuth developed the same large zinc grain size as the equivalent addition of 1.0% Pb. Thallium also had a significant enlarging influence whereas the effect of tin was relatively minor by comparison. The other additions were of still less significance in this regard.

(a) Non-Reactive Additives

The results in Table I indicate that aluminum, cadmium, magnesium, nickel, silver, vanadium, and zirconium did not cause separation of the zinc layer. As applicable with lead-free coatings, the zinc remained in intimate contact and was gradually consumed to form iron-zinc alloy. However, with 1.0% Pb also present, heating caused the zinc to separate in the same manner as with the coatings containing lead only. The separation reaction times were also similar.

It is noteworthy that the time required for complete disappearance of the zinc layer from the lead-free alloyed coatings was variable in some cases. For example, the period was significantly increased from 16 to 24 hours at 300°C (570°F) for the 4-minute coatings containing silver and nickel and for the 1-minute coating alloyed with vanadium. This is consistent behaviour even though opposing reaction effects were apparently involved. On the one hand, nickel, and vanadium more so, suppress the iron-zinc reaction rate. Retention of this inhibition was presumably maintained during heating to account for the slower rate of dissolution of the zinc layer. Silver, on the other hand, markedly accelerates iron-zinc alloy growth during galvanizing. Because of the increased coating thickness (longer diffusion path) the time for all of the zinc to react would again be extended.

The nickel-alloyed coatings were of special interest because of inter-metallic compound formation in the zinc layer and of the uniformly thin ζ phase formed during galvanizing. Typical coatings containing 0.2% Ni, with and without 1.0% Pb, are shown in Figure 16. In the lead-free case, gradual disappearance of the zinc layer exposed the compounds which otherwise remained keyed in place at the stage shown in Figure 16(b). Smaller compound particles were entrained in the ζ phase fringe, apparently as a result of entrapment by the outward growth of the latter. In the leaded coatings in Figures 16(c) and (d), the usual separation of the zinc layer is again well defined. The process was unaffected by the compounds present but to what extent growth or re-solution of the particles occurred during heating is unknown. This applied also with the lead-free coatings. With both series, a significant feature was the good resistance to intergranular fissuring of the ζ layer despite its well-defined columnar structure. Coincidentally, this layer decreased in thickness with time at an even rate and the characteristic uniformity originally evident was retained at all stages through the longest test of 2 weeks tried at 300°C (570°F).

(b) Reactive Additives

The low-melting-point additives, bismuth, indium, thallium, and tin, are all near to lead in the periodic table. As described in a previous section, thallium induced peeling just as lead did and this behaviour was duplicated by the others in the group. Except for indium, the separation end-point for the thicker series of coatings was, in fact, generally reached at an earlier stage than for the equivalent leaded coatings (Table I). Tin was most notable in this respect. When 1.0% Pb was also present, the influence of tin and indium remained unchanged, whereas the combination of bismuth and lead appeared to be somewhat beneficial in extending the time to separation. Tests were not attempted with leaded coatings containing thallium.

Microstructures of the 4-minute tin-containing coatings heated at 300°C (570°F) are illustrated in Figure 17. Complete separation of the zinc layer after less than 4 hours is well defined in Figure 17(b). Of particular note is the pronounced two-directional growth of the ζ phase, combining normal growth outwards as well as in the opposite direction towards the steel base. The δ_1 layer originally present was almost completely consumed in the process. The same effects were reproduced in the thicker coatings, although, at the end-point of the δ_1 - ζ transformation, a significant thickness of the former was retained. These indications of an enhanced reaction rate due to tin are clearly compatible with the observed earlier onset of zinc layer separation.

Several instances of similar sacrificial reciprocity involving δ_1 growth at the expense of Γ, and between the layers of the duplex-Γ structure, have already been mentioned. The former effect was also reproduced in the present case as shown by the renewal of δ_1 growth and complete absence of Γ in Figure 17(c). At the later stage in Figure 17(d), Γ growth was again restored and thereafter it increased in thickness in a regular manner.

These collective observations are of interest because they reveal significant departures from the accepted mechanism of growth of the individual iron-zinc phases. It is generally considered that the layers grow in an uninterrupted, continuous manner that varies according to parabolic time laws. However, a continuous growth mode for the δ_1, Γ, and the secondary-Γ layer, is clearly not universally applicable as shown by the selective step-wise growth characteristics observed. Depending on the conditions, each of these in turn suffered partial re-solution thereby temporarily promoting preferential growth of the adjacent lower-iron phase. To what extent these mechanisms can be extrapolated to the galvanizing reaction itself remains to be established.

The more rapid failure rate of the tin-containing coatings was confirmed in tests made at 400°C (750°F). As an example, Table I shows that 20-minute coatings required only 0.5 hours to reach the separation end-point as compared to 2 hours for those with 1.0% Pb only. This complete series was further

distinguished by significant thinning of the outer zinc layer before it was detached. With the 1-minute coatings in particular, separation was only evident at locally thicker patches of zinc still remaining. Such accelerated disappearance of the zinc layer before and after formation of the interface gap was the principal feature distinguishing the unleaded and leaded series of tin-containing coatings.

Typical bismuth-containing coatings are illustrated in Figure 18. The rapid zinc-layer separation at 300°C (570°F), duplicating that of tin, can be seen in Figure 18(b). In contrast, the iron-zinc alloy transformations found with tin were conspicuously absent and the rate of zinc loss after separation was much slower. Prolonged heating also failed to produce the temporary δ_1 or Γ re-solution effects observed with tin. The Γ phase showed particularly steady growth throughout heating periods of up to 2 weeks; this was interrelated with restricted formation of the "coherent" high-iron δ_1 needles. Regular iron-zinc alloy growth was similarly observed with the full range of coatings tested at 300°C (570°F) and also at 400°C (750°F). The metallographic evidence thus failed to account for acceleration of the separation process by bismuth.

The somewhat better resistance to peeling with both bismuth and lead present was also indeterminate, inclusive of coating thickness variations which were minor (Table I). In this series, the normal, columnar ζ phase layer was replaced by an equiaxed crystallite structure as shown in Figure 18(c). Because of its loose packing, the latter would be expected to be more prone to intergranular fissuring and to rapid separation of the zinc layer. That this was not the case was exemplified by the lead-free and leaded coatings in Figure 18(b) and (d), respectively; the measured time to separation was twice as long with the latter. Similar differences are defined in Table I for the other coatings in these two series.

Determination of the critical amounts of bismuth, indium, thallium, and tin that would cause peeling and of the effect of heating just above and below the melting points were not attempted. By analogy with lead and by the foregoing metallographic evidence, it can be assumed that melting of the respective constituents at the interface was not a primary factor in separation.

A further matter for speculation concerns the possible influence of the larger atomic size of these elements with respect to zinc (Bi-3.7, In-3.1, Pb-3.5, Sn-3.2, Th-3.4, Zn-2.8Å). If present substitutionally in the zinc, they could be expected to cause appreciable lattice distortion and thereby to affect the diffusion of zinc to the reacting interface. For this to be significant, an associated requirement must be satisfied, namely, some degree of solid solubility in zinc. This appears to be minimal, except perhaps with indium and tin (Bi-nil, In-<0.1%, Pb - < 0.0002%, Sn - 0.05%, Th-unknown). Therefore, until a more positive interrelationship between these parameters can be established, the role of atom size on the separation process remains uncertain. It may be noted that, of those alloying additions not causing separation,

only magnesium is atomically as large as the elements in the above group (3.2Å). All the others vary only fractionally above or below the value for zinc.

Duplex-Γ Layer

Several references have been made to the so-called duplex-Γ structure found in the coatings heated at 400°C (750°F). This took the form of two thin layers between the δ_1 and the steel base instead of the single Γ layer usually observed. The existence of this structure at such a low temperature has not been heretofore reported. Its occurrence in normal galvanized coatings is also apparently uncommon although it has been observed [27,28] with relatively long immersion times up to 1 hour in the galvanizing temperature range of 460-515°C (860-960°F).

No information is available on the identity and chemical composition of the secondary layer adjacent to the steel surface. It is nevertheless assumed to be the α solid solution of zinc in iron [29]. This is based in part on metallographic evidence presented by others [30-33] in which a two-phase eutectoidal mixture of $\alpha + \Gamma$ has been observed at temperatures above 570°C (1060°F). However, none of the available literature conclusively establishes the existence of solid solution α at lower temperatures. In this connection, Allen et al [34] state that α could not be detected after "dissolution annealing" for up to 4 hours at a maximum test temperature of 542°C (1010°F).

Evidence of the secondary-Γ layer previously referred to in Figures 7, 11, and 15 is complemented by the additional long-time microstructures in Figures 19 and 20. Reference may also be made to earlier tests with continuous strip in which similar structures were observed [2]. In all cases, the secondary phase layer was distinguished by its dark-etching response, by irregular and uneven growth, by a well-defined boundary with the normal Γ phase, and by its tendency to penetrate the steel intergranularly. The layer frequently contained a random scattering of fine particles, believed to be inclusions or other steel base constituents. Otherwise, it appeared to have a single phase structure.

Figure 19 shows that microhardness of the layer was intermediate between that of the hardest phase (Γ) and of the steel base. From measurements on several samples, the average hardness was 340-370 DPH compared to 460-520 for Γ (Leitz Mini-tester, 15-g load).

Electron probe microanalysis was carried out according to techniques described elsewhere [35] and the results of a typical probe trace across the duplex-Γ structure is illustrated in Figure 20. This representative example highlights the significant difference in iron content between the two layers and the relatively abrupt gradient at the boundary. Within each layer, the iron level was more or less constant. The probe data corrected for

fluorescence and absorption effects yielded an average value of 22.8% Fe for the Γ layer; this is well within the quoted equilibrium composition range of 20.5 to 28.0%. In contrast, the dark-etching secondary layer was consistently and significantly higher with an average value of 29.8% Fe.

On this evidence, the secondary phase cannot be α (88-100% Fe) and might best be described as a higher-iron form of Γ. The fact that its iron content is higher than the accepted equilibrium limit suggests that the latter could be in error. Recently reported probe results by Jackel et al (33) show still greater discrepancies, widening the Γ composition range to 19.4 - 33.3% Fe. This marked extension at both ends was claimed to be related to use of high carbon (0.45%) steel. In any event, it appears that two different structural forms of Γ are possible. These can apparently vary in iron content, hardness, and etching behaviour in a manner analogous to the "coherent" and "palisade" layer constituents of the δ_1 phase. Also, as discussed earlier, the secondary - Γ layer showed temporary sacrificial reciprocity with the Γ layer, similar to that demonstrated by δ_1 in dissolving to form ζ under certain conditions (Figures 7, 11, and 17).

Practical, as well as academic, considerations would appear to warrant more intensive investigation of the identity and properties of this secondary-Γ phase. Apart from uniqueness, the question arises as to its possible existence in minute quantities during galvanizing, and to its potential effect on coating reactions and properties. Also, because of its characteristic tendency to penetrate the steel base intergranularly, it would appear to be of importance in galvanized product embrittlement. This applies to deterioration at elevated temperatures and possibly under other conditions as well.

SUMMARY AND DISCUSSION

The foregoing investigation has established that air-atmosphere heating of laboratory-produced conventional galvanized coatings in the temperature range of 275-400°C (525-750°F) resulted in two different deterioration modes.

The first was applicable to leaded coatings (>0.001% Pb) and was manifested by formation of a gap at the interface between the ζ phase and the outer zinc layer. The gap was caused by dissolution of the zinc in the interstices of the ζ phase fringe and widened with time along the entire interface. Reaction of the zinc thereafter continued at a reduced rate so long as the layer was neither disturbed nor lifted out of place. Presumably, diffusion transport of zinc atoms was maintained at points where the layer remained locally keyed. Identical failure mechanisms were produced by elements which are near to lead in the periodic table. Additions of 1.0% of In or Tl were as harmful as lead, whereas 1% of Bi or Sn accelerated the separation reaction. When these or other alloying additions were combined with 1.0% Pb, the basic separation process occurred in all cases.

The second mode applied to lead-free coatings (<0.001% Pb). Heating deterioration in this case, subsequently confirmed by other investigators (6), involved uninterrupted inward diffusion of the zinc layer, until it was completely used up. At no stage was there any evidence of bond failure at the Zn-ζ interface. Cavity formation of any note was also minimal except in the special case of the open fan-like ζ structure at corners and curved surfaces. When the coating was alloyed with individual additions of 0.1% of Al, V or Zr, 0.7% Ag, 1.0% Cd, 0.06% Mg, or 0.2% Ni, the basic behaviour of lead-free coatings was reproduced. Notably, the rate of dissolution of the zinc layer was slowed down in varying degrees by nickel, silver, vanadium and zirconium, with vanadium being most effective.

Apart from coating composition and time and temperature parameters, the reaction rate with both mechanisms was found to be dependent on the coating thickness. Also confirmed was the practical observation that only relatively thin coatings should be susceptible to peeling failure on retarded cooling after galvanizing. Even this can be prevented by ensuring unrestricted heat dissipation for the first few minutes after galvanizing. The separation mode was further established to be unrelated to such factors as grain size of the outer zinc layer and the melting point and atomic size of the coating alloying additions tried. Accumulation of a barrier layer of lead at the interface and oxidation phenomena in this region could similarly be discounted.

Other noteworthy microstructural changes occurring during heating were observed. With lead-free coatings, for example, iron-zinc alloy transformations were sustained at a high rate, most probably because all of the zinc in the outer layer remained available for reaction. On the other hand, where the separation mode applied, the zinc supply was largely cut-off, thereby reducing the subsequent rate and amount of iron-zinc alloy growth. This reaction difference would appear to have practical application in the field of galvannealed coating production. Transforming the outer zinc layer to iron-zinc alloy is the basis of this process, and the possibility of increasing the reaction rate by the use of low-lead starting strip appears to be worthy of further investigation.

The characteristic sacrificial reciprocity noted between bounding iron-zinc phases under certain conditions suggests that the accepted mode of growth of the individual layers requires reconsideration. Because this bears directly on the diffusion kinetics of the iron-zinc reaction, more extensive study in this area appears to be warranted. This applies as well to the formation of a structurally unique high-iron phase layer next to the steel base which was identified by metallographic and electron probe analysis and designated as secondary Γ. The layer is of further interest because of its direct association with galvanized-coating embrittlement phenomena.

The peeling deterioration process in conventional galvanized coatings is an apparently complex phenomenon owing to its diffusion dependence and to

the multi-phase nature of the system. A complete explanation is still largely speculative because none of the mechanisms advanced for bond failure at the Zn-ζ interface can account for all of the observed facts. The more important of these mechanisms and an alternative explanation suggested by the experimental findings are discussed below.

(a) Kirkendall Effect

Hershman et al [5] concluded that separation was related to the Kirkendall effect whereby lattice vacancies migrate and collect at the Zn-ζ interface owing to zinc being the faster diffusing species. This follows the accepted explanation for void formation in metallic diffusion couples and is most consistent with respect to the depletion of zinc bordering and forming the intercrystalline matrix of the ζ layer. The faceted undercutting on the bottom of the separated layer must then be assumed to be due to zinc-dissolution enlargement of the primary separation voids by surface diffusion, vapor transport, oxidation corrosion, or some other mechanism. This secondary stage is really not relevant to the actual separation reaction other than to account, in part, for the gradual disappearance of the zinc layer after it has separated.

On the other hand, if Kirkendall condensation of lattice vacancies is basically responsible, it remains to be explained why there is also preferential migration of vacancies in the opposite direction to cause the surface pitting observed. This was the primary reaction effect on heating, being most pronounced with thin coatings and much less so as the coating thickness (diffusion path length) increased. It is possible that random vacancy movement to the surface and to the Zn-ζ interface at the same time is an inherent characteristic of the system, particularly with a short diffusion path as in thin coatings. However if this behaviour is real, the zinc layer separation process cannot be said to conform exactly to the Kirkendall mechanism laws. This is of practical importance because it implies that separation may not be entirely diffusion-dependent and, therefore, inherently unavoidable at elevated temperatures. That separation can in fact be completely avoided was clearly demonstrated by coatings relatively free of lead and the low melting-point elements, bismuth, indium, thallium, and tin.

It is important to note that even minute traces of impurity and alloying additions can affect the properties of lattice defects, notably with respect to an increase in the density of dislocations. It is also well established that lattice vacancies can preferentially migrate to form "atmospheres" around dislocations and can be attracted to substitutional atoms that differ appreciably in size from the surrounding lattice. Coalescence of vacancies at the interface between insoluble constituent particles and the matrix is another possibility. The end result can be a change in the rate of diffusion in the system.

These phenomena suggest an alternative explanation for the separation process. If the alloying elements in question can impede diffusion feeding of zinc to the reaction interface, the zinc reacting to form iron-zinc alloy cannot be replenished as fast as it is used up. This region would then become impoverished in zinc, resulting in formation of the characteristic interface gap. Random lattice vacancy movement in the zinc layer is implicit in this mechanism, being dependent on the form and distribution of the foreign elements and on the lattice defects thereby introduced. With such movement, the surface pitting effects observed in early stages of heating can be accounted for, as can also the subsequent angular indenting on the underside of the zinc layer. Neither of these effects are compatible with the Kirkendall mechanism which requires a predominantly unidirectional movement of vacancies to the separation interface. This arises from the assumption, still not conclusively established otherwise, that zinc is the faster diffusing species in the iron-zinc couple.

Over and above all else, the Kirkendall mechanism fails to account for the lack of zinc layer separation with lead-free coatings. These would in fact be expected to be more amenable to operation of a Kirkendall couple because of the higher purity of the system and therefore less interference with diffusion movement of the reactants. Since the reverse applies, namely, that interface cavities do not form, there would appear to be some uncertainty about the idea of a preferentially higher rate of diffusion by zinc in the iron-zinc couple. It is therefore concluded that the alternative mechanism proposed, which involves restricted diffusion of zinc to the Zn-ζ interface and subsequent zinc impoverishment in this region, offers a more consistent explanation for the zinc peeling process.

(b) Differential Expansion

The threefold difference in coefficient of expansion of zinc and iron is not infrequently quoted as the cause of peeling [14, 15]. This has the major objections that separation is primarily dependent on coating thickness and the time and temperature of heating. It also fails to consider the marked anisotropy in thermal expansion exhibited by zinc, coupled with the variable crystallographic orientation of the grains in the zinc layer.

Previous work [1-2] has shown that the expansion and contraction stresses induced by cyclic heating and cooling of continuous strip coatings were relieved by plastic deformation and by cleavage and grain boundary cracking within the zinc layer. Separation of the layer did not occur until a later stage and was confined to sites of the localized iron-zinc alloy nodules which formed during prolonged heating. Excessive elongation of the zinc overlying the growing mounds was, in large part, responsible for bond failure at these sites. With conventional coatings, expansion of the zinc layer could be involved in separation to the extent of triggering the process after the interface

bond had been weakened by the diffusion voids formed. Such a secondary shearing-stress action has been proposed as a factor contributing to spalling of aluminized coatings (17). It could account for the "popping" type of failure illustrated in Figure 2.

(c) Internal Stresses

An alternative peeling explanation is suggested by the extensive vertical cracking and faulting observed, particularly in thicker coatings. The cracks originate in the δ_1 layer which is suggestive of a condition of high internal stress therein. This is to be expected because of its volume growth characteristics (36) and the constraint imposed by the covering ζ layer. Twinning effects observed in the δ_1 are also indicative of a stress condition (37). Furthermore in the coating system as a whole, a stress imbalance would be highly probable because of its multi-component nature and the different crystallographic properties, growth characteristics, chemical composition, and expansion properties of the individual layers.

It could therefore be speculated that the combination of these factors might be instrumental in promoting separation at the Zn-ζ interface because it is apparently the weakest boundary in the system; it could be considered as offering the minimum bulk resistance to shearing. However, the influence of an internal stress mechanism is uncertain if for no other reason than the limited cracking evident in thin coatings which were most prone to rapid peeling failure. Moreover, it again cannot account for the freedom from separation with the lead-free coatings in which all the stress factors in question would be equally operative.

CONCLUSIONS

Conventional galvanized coatings containing <0.001% Pb or otherwise separately alloyed with 0.1% of Al, V or Zr, 0.7% Ag, 1.0% Cd, 0.06% Mg, or 0.2% Ni, did not exhibit any peeling of the outer zinc layer when heated within the temperature range of 275-400°C (525-750°F).

Peeling of the zinc layer was induced when the coatings contained >0.001% Pb or were separately alloyed with 1.0% of Bi, In, Sn or Tl.

The rates of both reaction modes were primarily dependent on the time and temperature of heating and the coating thickness.

The mechanism of the peeling mode of failure appears to involve a restriction on diffusion feeding of zinc to the reaction interface. Consequent impoverishment of zinc in this region results in formation of the interface gap and separation of the zinc layer remaining.

There were indications that the iron-zinc alloying reaction rate in galvannealed coating production might be beneficially increased by the use of low-lead galvanized strip.

In general galvanizing practice, the higher susceptibility of thin coatings to peeling failure can be minimized by ensuring unrestricted heat dissipation for the first few minutes after galvanizing withdrawal.

In the context of this investigation and the reaction effects examined, lead was indicated to be an undesirable additive to galvanized coatings. On the other hand, it will be appreciated that galvanized coatings find limited application at elevated temperatures. Therefore, the advantageous suppression of peeling to be achieved by limiting the lead content to <0.001% must be weighed against the recognized economic and technical advantages associated with leaded galvanizing baths. To what extent lead could be rendered innocuous in the area in question remains a matter for further investigation.

REFERENCES

1. J. J. Sebisty, R. H. Palmer and D. F. Watt - "The Elevated-Temperature Behaviour of Continuous-Strip Galvanized Coatings" - Physical Metallurgy Division Internal Report PM-R-63-13, Mines Branch, Department of Energy, Mines and Resources, Ottawa (1966).

2. J. J. Sebisty - "Continuous-Strip Galvanized Coatings at Elevated-Temperatures" - Electrochemical Technology 6(5), 330-336 (1968).

3. J. J. Sebisty - "The Properties of Galvanized Coatings at Elevated Temperatures" - Physical Metallurgy Division Internal Report PM-R-67-5, Mines Branch, Department of Energy, Mines and Resources, Ottawa (1967).

4. J. J. Sebisty and R. H. Palmer - "The Behaviour of Thick-Wall Galvanized Products at Elevated Temperatures" - Mines Branch Research Report R200, Department of Energy, Mines and Resources, Ottawa (1968).

5. A. A. Hershman and N. D. Neemuchwala - "The Peeling of the Zinc Layer in Galvanized Coatings" - British Corrosion Journal 1(2), 51-52 (1965).

6. Joint Discussion - ibid 1(5), 251 (1966).

7. M. L. Hughes - "The Formation of Hot Dipped Zinc Coatings" - Product Finishing 6(8), 49-62 (1953).

8. Joint Discussion - Proc. Second International Galvanizing Conference, Zinc Development Assoc. London, 40 (1952).

9. G. P. Lewis - private communication (1961).

10. J. J. Sebisty - "Metallurgical Examination of Galvanized Tubing" - Mines Branch Investigation Report IR 66-4, Department of Energy, Mines and Resources, Ottawa (1966).

11. Joint Discussion - Proc. Sixth International Galvanizing Conference, Zinc Development Assoc. London, 95 (1961).

12. Joint Discussion - Proc. Third International Galvanizing Conference, Zinc Development Assoc. London, 56-57 (1954).

13. R. Haarmann - "Problems in Practical Hot Dip Galvanizing" - Proc. Eighth International Galvanizing Conference, Zinc Development Assoc. London, 104-135 (1967).

14. H. Bablik, F. Götzl and E. Nell - "The Cooling of Galvanized Products" - Metall. 9(8), 643-645 (1955).

15. J. Teindl and O. Blahoz - "Causes of Peeling of Zinc from Galvanized Steel Sheet", Hutnicke Listy 21(3), 179-181 (1966).

16. K. S. Frazier - private communication (1964).

17. M. Tagaya, S. Isa and Y. Onoe - "Phenomena Produced on Heating Aluminized Steel" - Jnl. Metal Finishing Soc. (Japan) 12(11), 443-446 (1961).

18. T. Saga - "Behaviour of Aluminized Coatings on Heating" - Nippon Kingoku Gakkaishi (Japan) 22(4), 177-180 (1958).

19. J. J. Sebisty - "Hot Dip Galvanizing with Less Common Bath Additions" - Proc. Seventh International Galvanizing Conference, Zinc Development Assoc. London, 235-265 (1964).

20. D. H. Rowland - "Metallography of Hot-Dip Galvanized Coatings" - Trans. Am. Soc. Metals 40, 983-1011 (1949).

21. G. Bassi and J. P. Hugo - "Etch Pits in Zinc" - Jnl. Inst. Metals 87, 376-379 (1958-59).

22. G. B. Rais and M. I. Bromberg - "Vacuum Thermal Etching of Twinned Zinc Monocrystals" - Soviet Physics; Crystallography 4, 555-557 (1960).

23. R. Kamel - "Natural Pitting on Cleaved Surfaces of Zinc Crystals" - Acta Metallurgica 11, 629-630 (1963).

24. P. E. Doherty and R. S. Davis - "The Formation of Surface Pits by the Condensation of Vacancies" - Acta Metallurgica 7, 118-123 (1959).

25. R. H. Palmer and H. R. Thresh - "Electron Probe Microanalysis of Heat-Treated Conventional Galvanized Coatings" - Physical Metallurgy Division Internal Report PM-R-69-14, Mines Branch, Department of Energy, Mines and Resources, Ottawa (1969).

26. A. A. Hershman - private communication (1967).

27. A. A. Hershman - "Alloy Formation in Hot Dip Galvanizing" - Proc. Seventh International Galvanizing Conference, Zinc Development Assoc. London, 189-208 (1967).

28. H. Bablik - "The Reaction of Zinc and Iron in Hot-Dip Galvanizing" - Metal Finishing, 585-586 (1940).

29. D. Horstmann and F. K. Peters - "The Reactions Between Iron and Zinc" - Proc. Ninth International Galvanizing Conference, Zinc Development Assoc. London, 75-106 (1970).

30. S. E. Hadden - "Effect of Annealing on the Resistance of Galvanized Steel to Atmospheric Corrosion" - Jnl. Iron and Steel Inst. 171(6), 121-127 (1952).

31. W. Katz - "Structure and Heat Treatment of Galvanized Coatings" - Metall 9 (8), 652-655 (1955).

32. W. N. Brown and J. Mackowiak - "Kinetics of Interaction Between Iron and Zinc" - Corrosion Science 5, 779-785 (1965).

33. G. Jackel, H. E. Buhler and L. Meyer - "The Iron-Zinc-Carbon Ternary System" - Proc. Ninth International Galvanizing Conference, Zinc Development Assoc. London, 107-126 (1970).

34. C. Allen and J. Mackowiak - "Influence of Intermetallic Iron-Zinc Layers on Rates of Attack of Solid Iron by Liquid Zinc" - Corrosion Science 3, 87-97 (1963).

35. J. J. Sebisty, R. H. Palmer and H. R. Thresh - "Electron Probe Microanalysis of Alloyed Galvanized Coatings" - Proc. Ninth International Galvanizing Conference, Zinc Development Assoc. London, 152-170 (1970).

36. W. Koster - "The Ternary System Iron-Silicon-Zinc" - Metallurgia 80, 219-229 (1969).

37. H. Bablik - "Hot-Dip Galvanizing" - 3rd Edition, Spon, London (1950).

- - - - -

JJS/DP/gm

TABLE I

Coating Test Results*

Nominal Bath Additions (%)			Reaction Mode		Reaction Time (hr)								Coating Weight ** (oz. sq ft-sheet)			
					275°C (525°F)		300°C (570°F)				400°C (750°F)							
Pb	Fe	Others	Zinc Layer Separated	Zinc Layer Diffused	(1)	(4)	(1)	(4)	(10)	(20)	(1)	(4)	(10)	(20)	(1)	(4)	(10)	(20)
<.001	.03	-		x	24	36	8	16	24	48	.75	1.5	2	2.5	1.91	2.71	3.52	4.74
.0015	"	-	x				4	8							1.90	2.35		
.003	"	-	x				4	8							1.89	2.45		
.006	"	-	x				4	8							1.89	2.72		
.01	"	-	x				4	8							1.85	2.45		
.06	"	-	x				4	8							1.87	2.55		
.1	"	-	x				4	8							1.86	2.75		
.2	"	-	x				4	8							2.02	2.79		
.3	"	-	x				4	8							1.93	2.82		
1.0	"	-	x		12	24	4	8	16	24	.08	.5	1.5	2	1.86	2.68	3.88	4.81
-	"	1.0 Bi	x				4	4	8	16	.08	.5	.5	1	1.92	2.49	3.51	4.76
1.0	"	"	x				8	16	24	24					2.08	2.62	3.62	4.65
-	"	1.0 In	x				4	8	16	24					1.68	2.44	3.39	4.29
1.0	"	"	x				4	8	16	24					1.93	2.98	4.0	4.59
-	"	1.0 Sn	x				<2	<4	4	4	.08	<.5	.5	.5	1.73	2.54	3.34	4.25
1.0	"	"	x				<2	<4	<8	8	.08	<.5	.5	.5	1.81	2.71	3.54	4.55
-	"	1.0 Tl	x				4	8	8	24					-	-	-	-
.	"	.7 Ag		x			8	24							2.42	4.2		
1.0	"	"	x				8	16							2.52	3.7		
-	"	.1 Al		x			8								1.7			
-	"	1.0 Cd		x			8	16	24	48					1.81	2.56	3.58	4.8
1.0	"	"	x				4	8	16	24					1.94	2.96	4.12	4.65
-	"	.06 Mg		x			8								1.82			
1.0	"	"	x				4								1.92			

TABLE I (Cont'd.)

Coating Test Results*

Nominal Bath Additions (%)			Reaction Mode		Reaction Time (hr)										Coating Weight ** (oz/sq ft-sheet)			
					275°C (525°F)		300°C (570°F)				400°C (750°F)							
Pb	Fe	Others	Zinc Layer Separated	Zinc Layer Diffused	(1)	(4)	(1)	(4)	(10)	(20)	(1)	(4)	(10)	(20)	(1)	(4)	(10)	(20)
-	.03	.2 Ni		x			8	24							1.51	2.35		
1.0	"	"	x				4	4							1.54	2.45		
-	"	.1 V		x			16								1.34			
1.0	"	"	x					4								1.90		
-	"	.1 Zr		x			8	16							1.50	1.95		
1.0	"		x				4	4							1.65	2.0		

* Heating test periods - at 275°C (525°F): 1, 3, 5, 8 and 12 hours; 1, 2, 3 and 8 days.
- at 300°C (570°F): 2, 4 and 8 hours; 1, 2, 7 and 14 days.
- at 400°C (750°F): 5, 10, 20, 30, 45 and 60 minutes for 1- and 4-minute coatings.
: 0.5, 1. 1.5, 2, 4 and 48 hours for 10- and 20-minute coatings.

Bracketed column headings indicate galvanizing immersion time in minutes.

** 1 oz/sq ft = 305 g/m^2

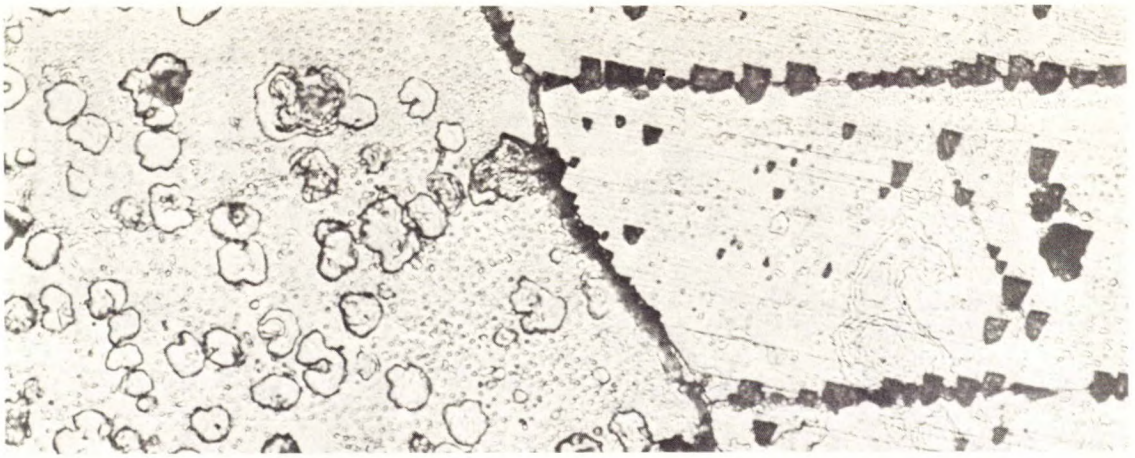

(a) One-minute coating after 5 hours at 275°C (525°F).

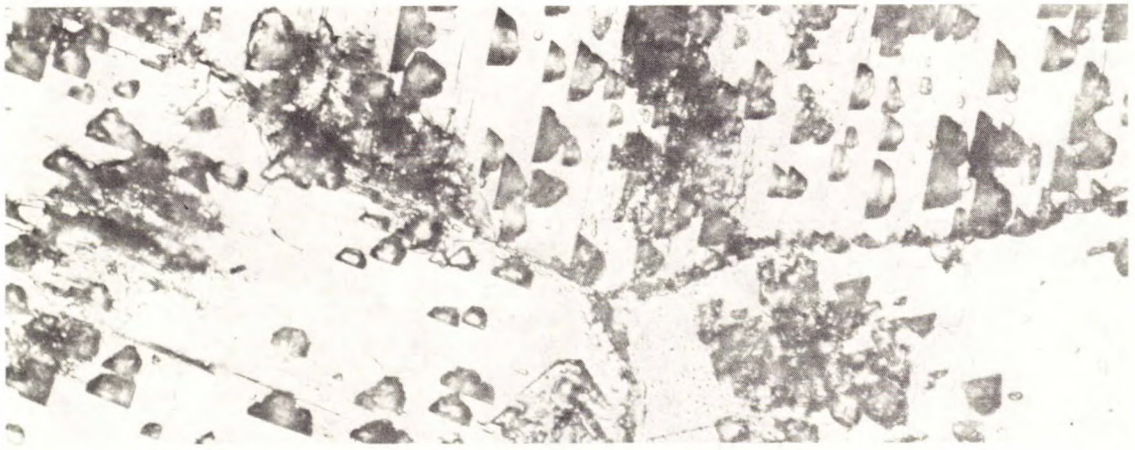

(b) One-minute coating after 12 hours at 275°C (525°F).

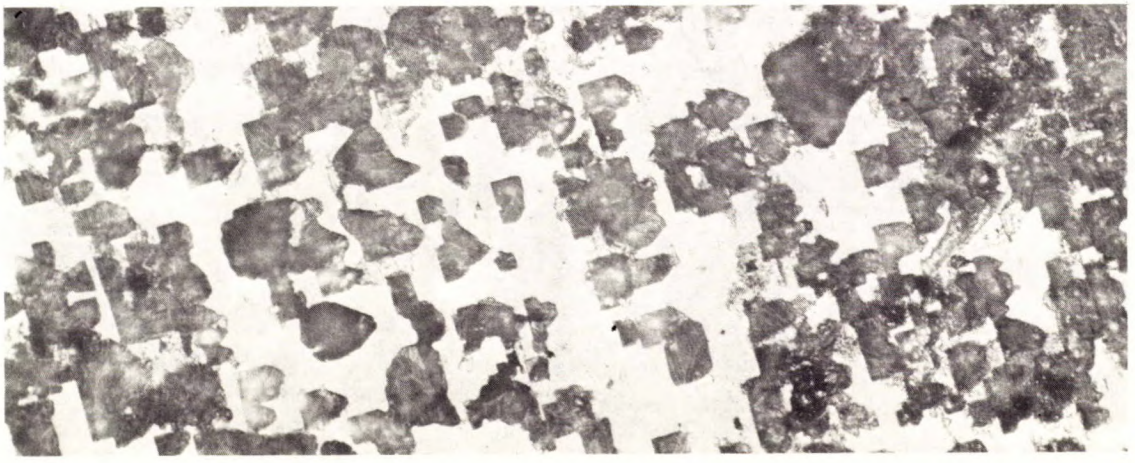

(c) Ten-minute coating after 8 days at 300°C (570°F).

Figure 1. Surface pitting on coatings containing 1.0% Pb. X300

Figure 2. Peeling and break-up of coating (0.5% Pb, 0.10% Al, 1.20% Sn, 0.30% Cd, 0.30% Cu, 0.03% Fe) after heating for 16 hours at 335°C (635°F). X3

(a) Surface pitting around local iron-zinc alloy growth. X300

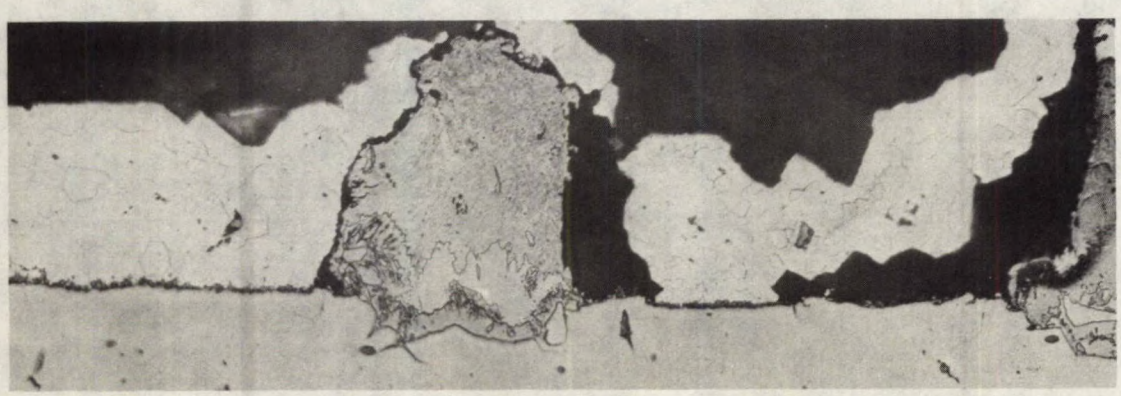

(b) Cross-section of growth in (a) X500

Figure 3. Continuous-strip coating heated for 1 week at 300°C (570°F). X500

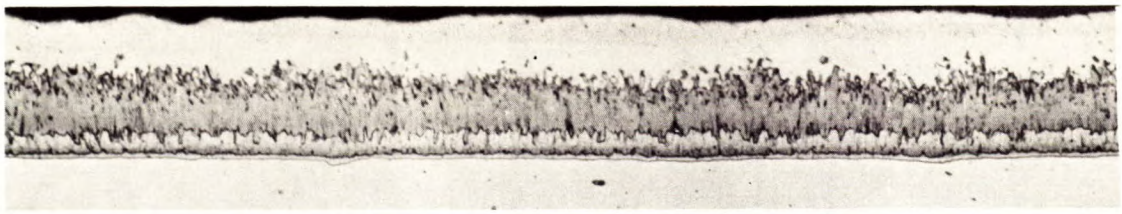

(a) As-galvanized (1.86 oz/sq ft)

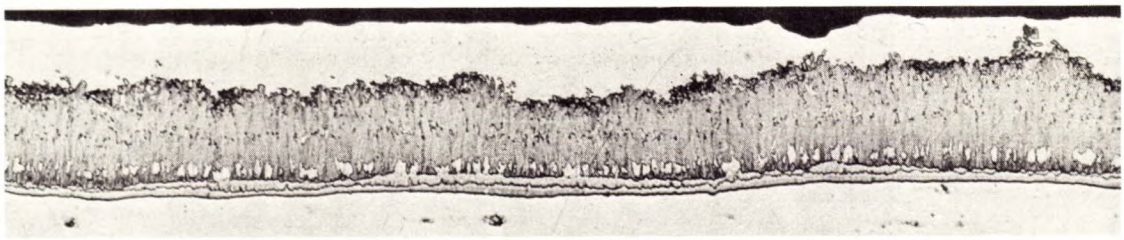

(b) 5 hours

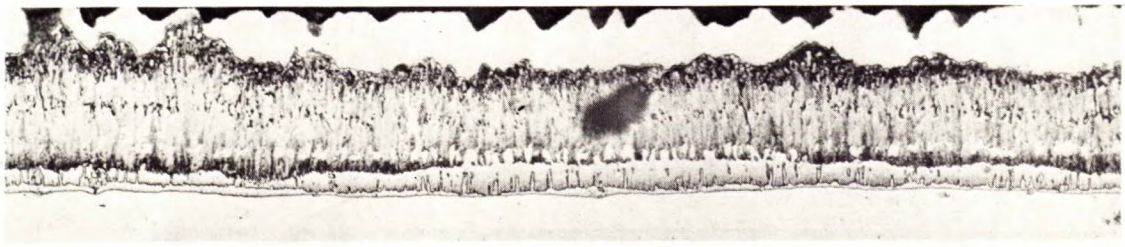

(c) 12 hours

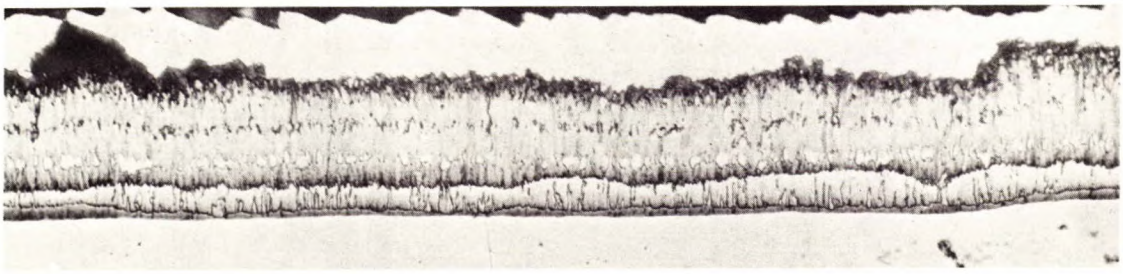

(d) 1 day

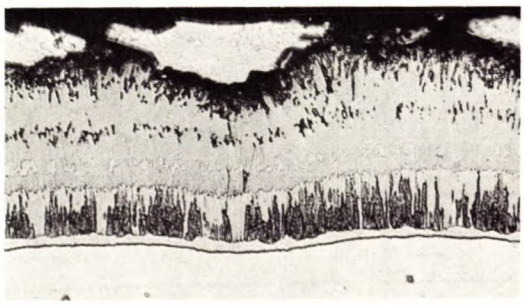

(e) 2 days

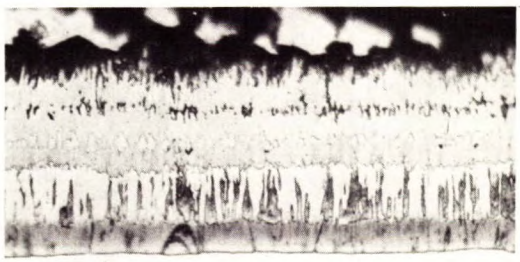

(f) 8 days

Figure 4. One-minute leaded coatings (1.0% Pb) heated at 275°C (525°F). X500

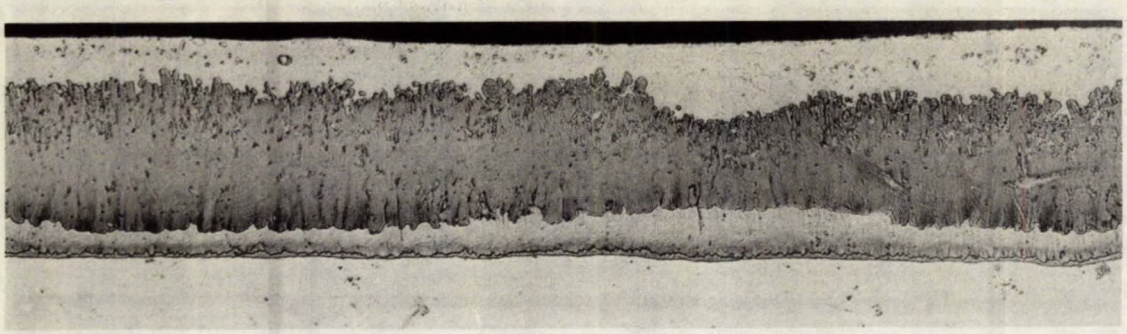

(a) As-galvanized (2.68 oz/sq ft)

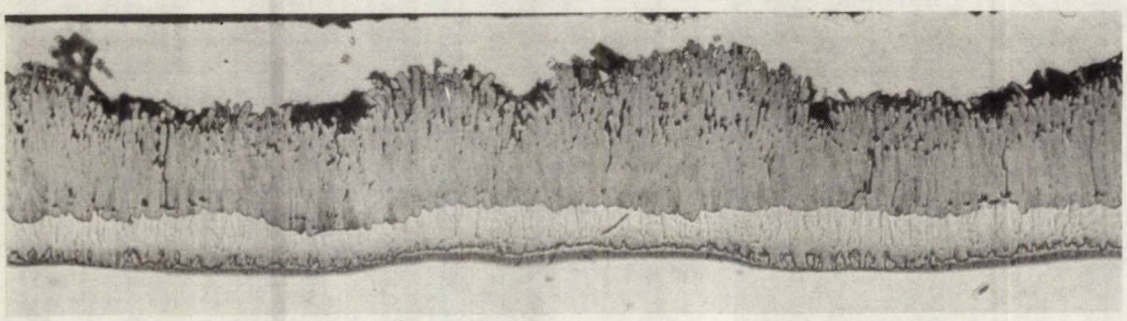

(b) 12 hours

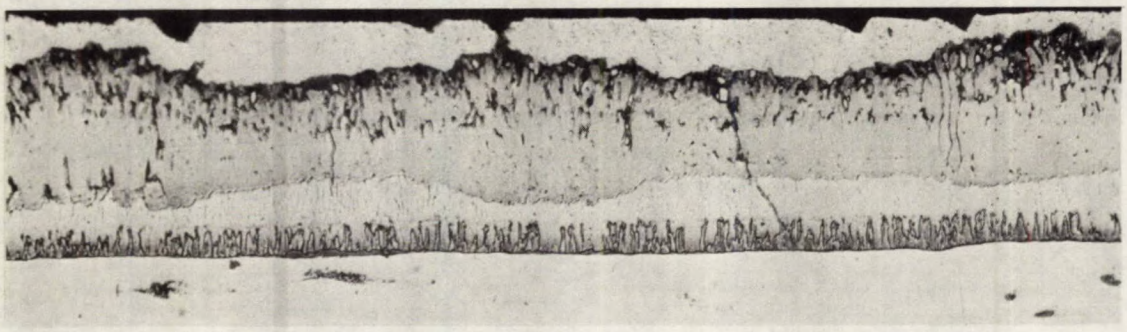

(c) 1 day

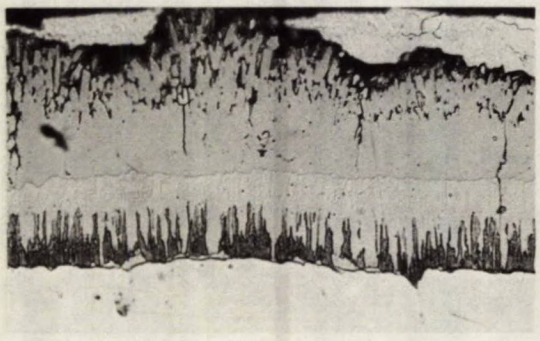

(d) 2 days

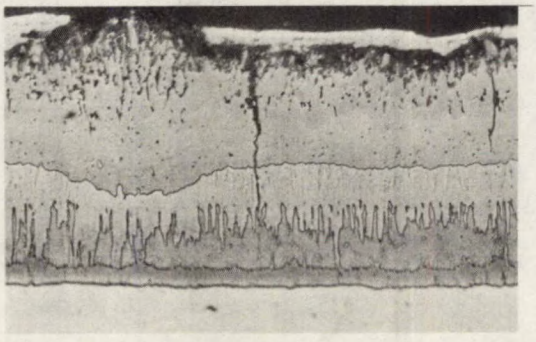

(e) 8 days

Figure 5. Four-minute leaded coatings (1.0% Pb) heated at 275°C (525°F).
X500

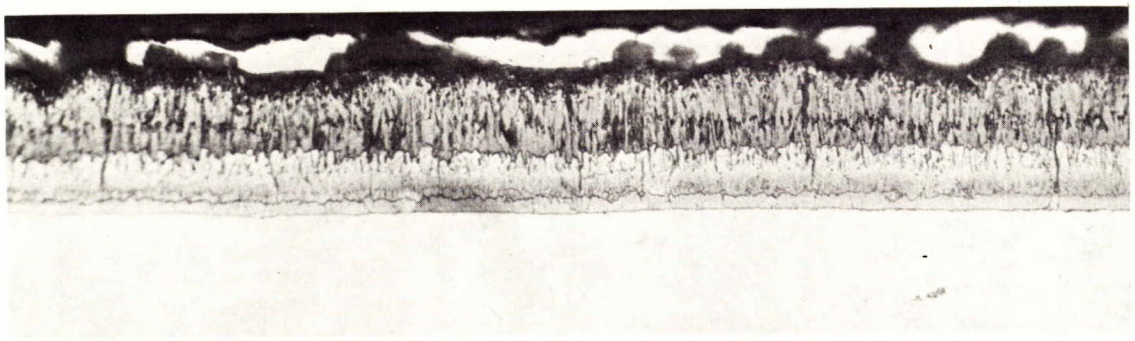

(a) One-minute coating

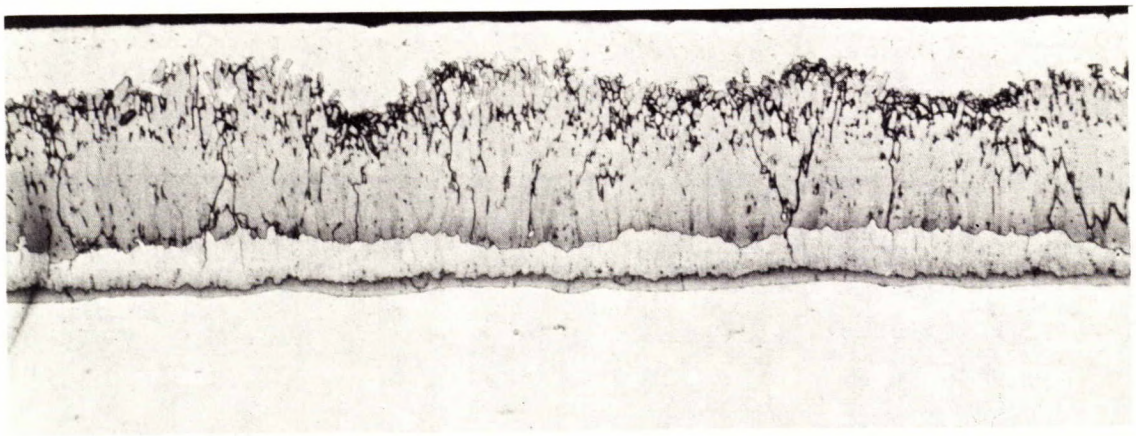

(b) Four-minute coating

Figure 6. Leaded coatings (1.0% Pb) heated for 30 minutes at 400°C (750°F). X500

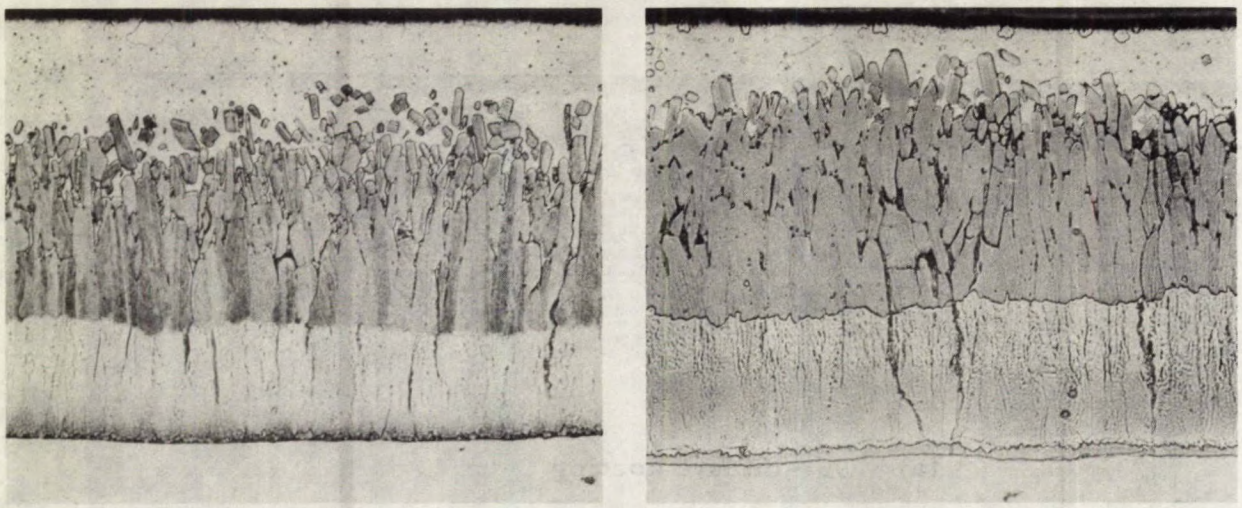

(a) As-galvanized (4.81 oz/sq ft) (b) 1 hour

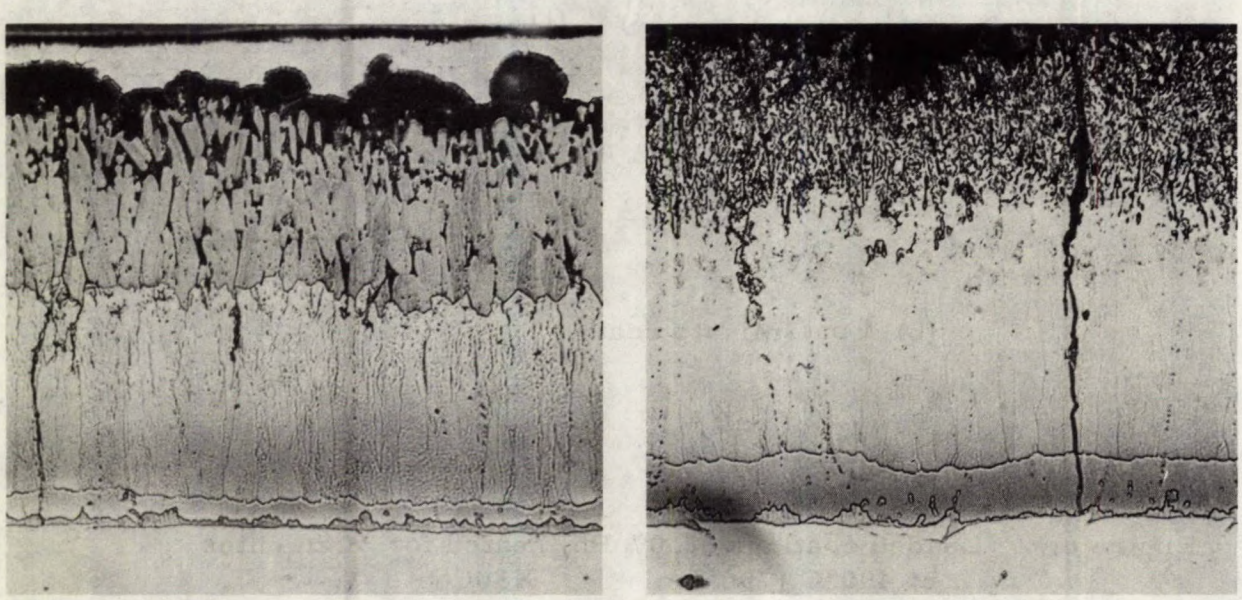

(c) 4 hours (d) 2 days

Figure 7. Twenty-minute leaded coatings (1.0% Pb) heated at 400°C (750°F). X500

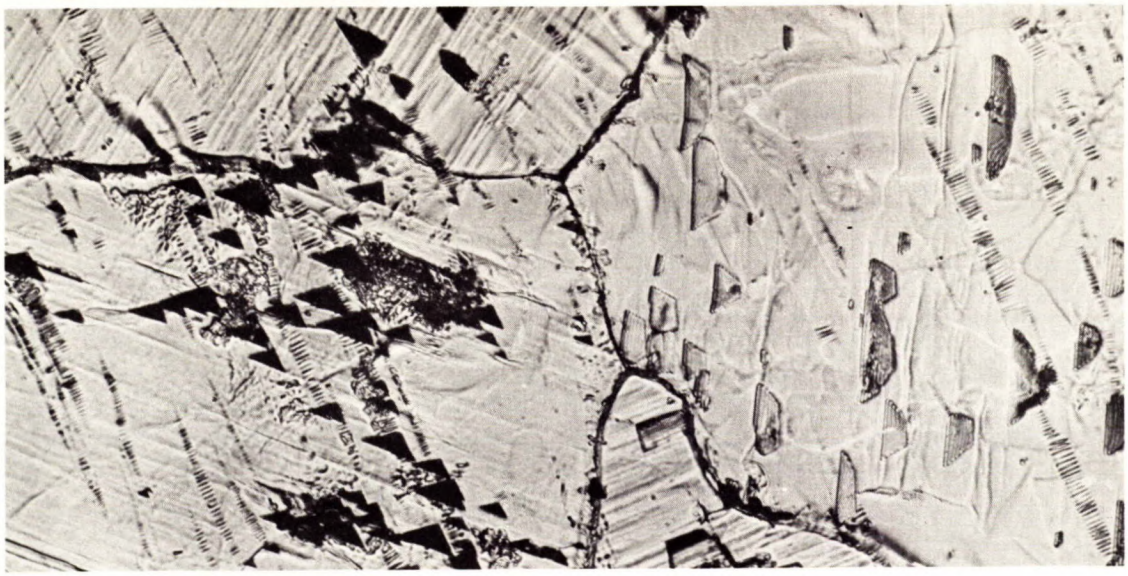

(a) 5 hours

(b) 12 hours

Figure 8. Surface pitting and zinc depletion on 1-minute lead-free coatings (<0.001% Pb) heated at 275°C (525°F). X500

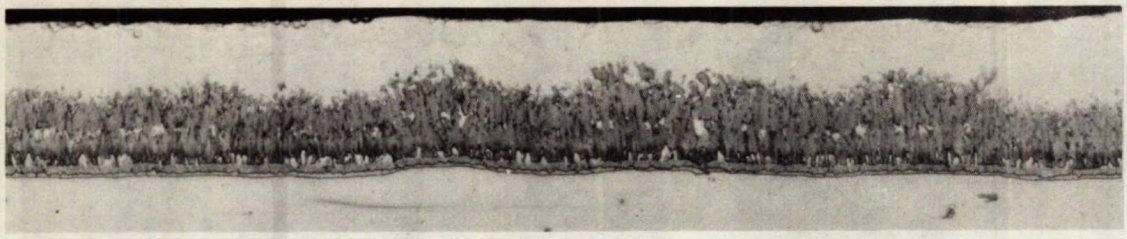

(a) As-galvanized (1.91 oz/sq ft)

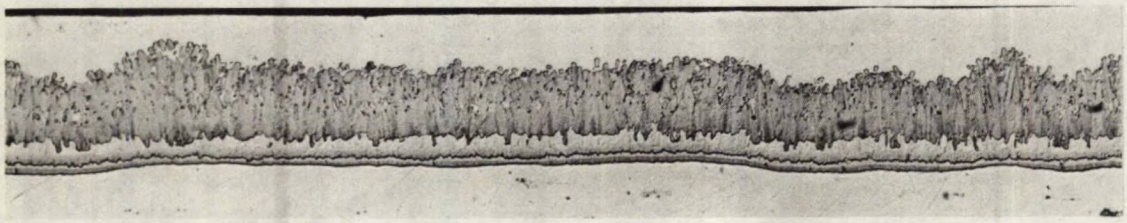

(b) 5 hours

(c) 12 hours

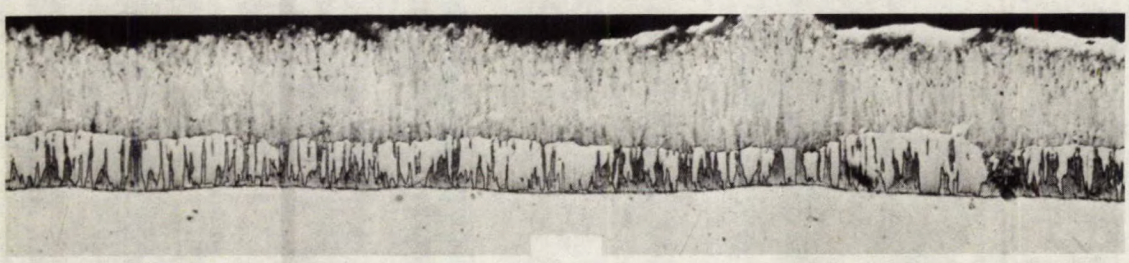

(d) 1 day

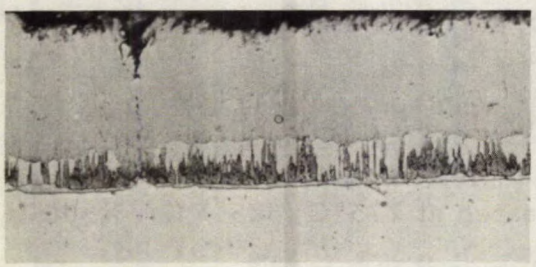

(e) 2 days

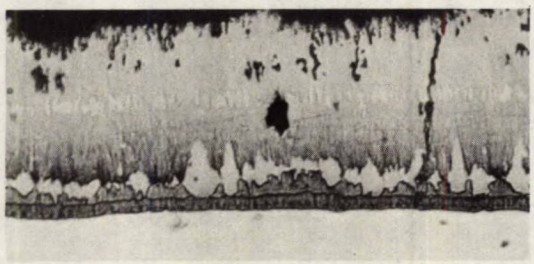

(f) 8 days

Figure 9. One-minute lead-free coatings (<0.001% Pb) heated at 275°C (525°F). X500

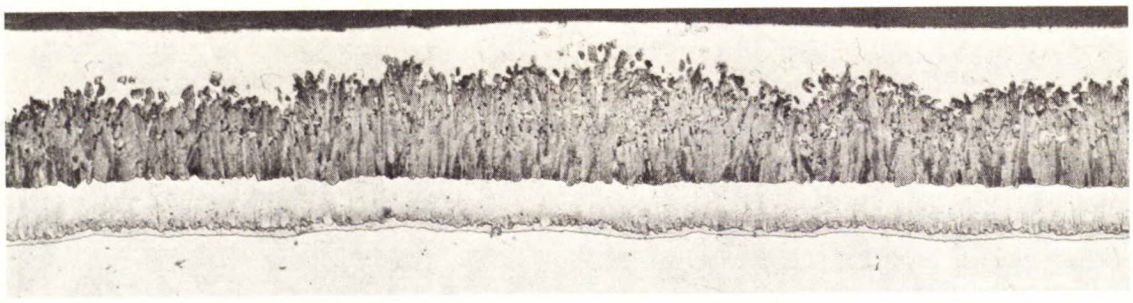

(a) As-galvanized (2.71 oz/sq ft)

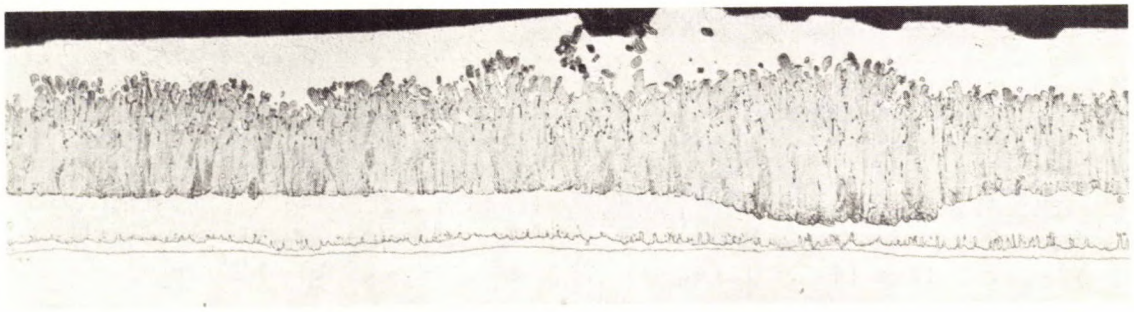

(b) 12 hours

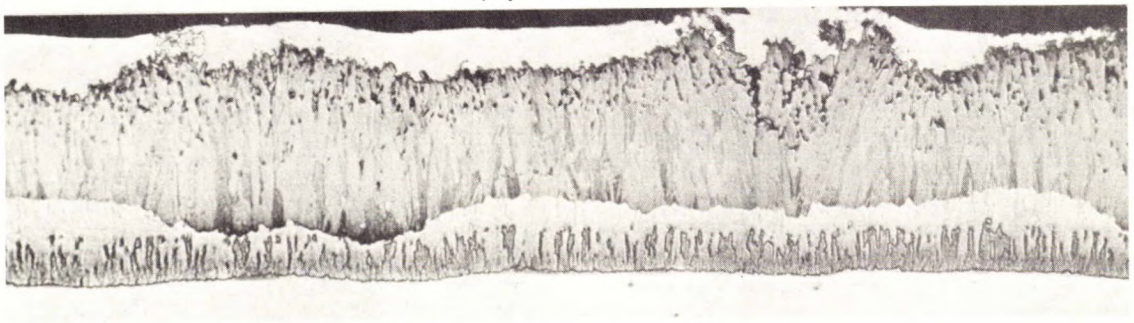

(c) 1 day

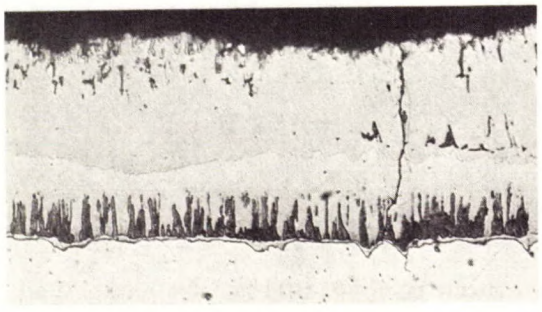

(d) 2 days

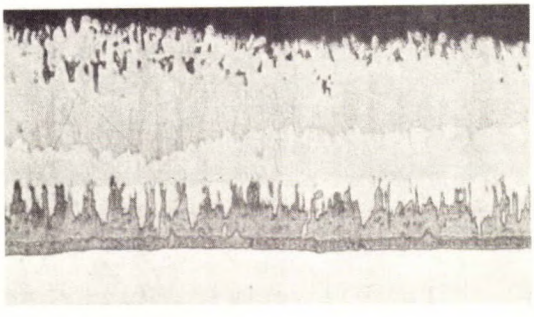

(e) 8 days

Figure 10. Four-minute lead-free coatings (<0.001% Pb) heated at 275°C (525°F). X500

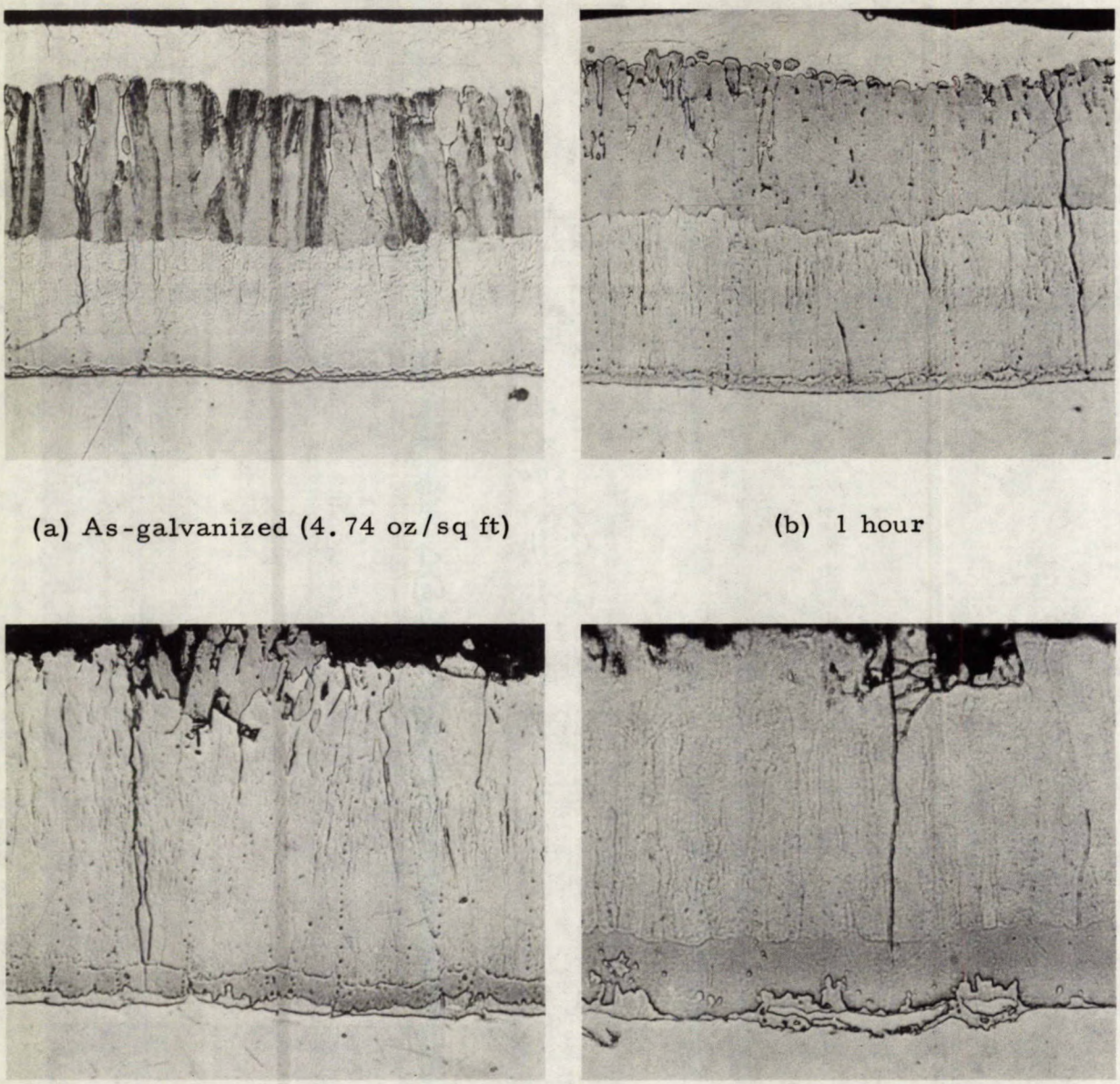

(a) As-galvanized (4.74 oz/sq ft)

(b) 1 hour

(c) 4 hours

(d) 2 days

Figure 11. Twenty-minute lead-free coatings (<0.001% Pb) heated at 400°C (750°F). X500

(a) Lead-free (<0.001% Pb)

(b) 0.003% Pb

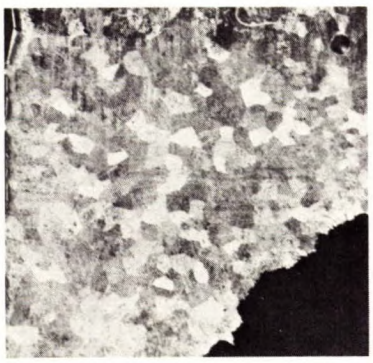

(c) 0.06% Pb

(d) 1.0% Pb

Figure 12. Surface appearance of 1-minute coatings with lead content indicated, after heating for 8 hours at 300°C (570°F). Dark corner patches are areas where zinc was peeled away. X1

(a) Lead-free (<0.001% Pb)

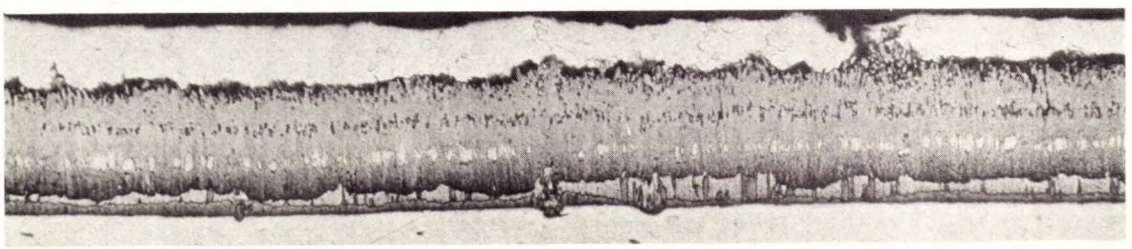

(b) 0.0015% Pb

Figure 13. Lead-free and low-lead coatings (1-minute immersion) after heating for 4 hours at 300°C (570°F). X500

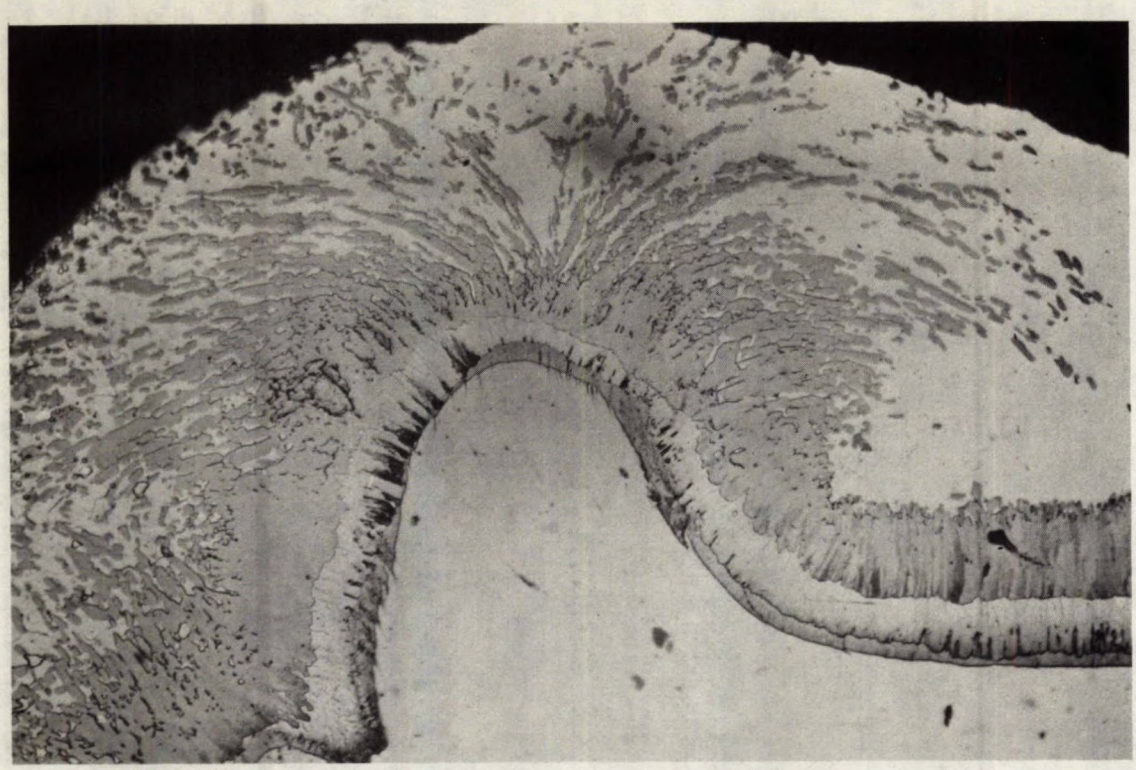

(a) Lead-free (<0.001% Pb)

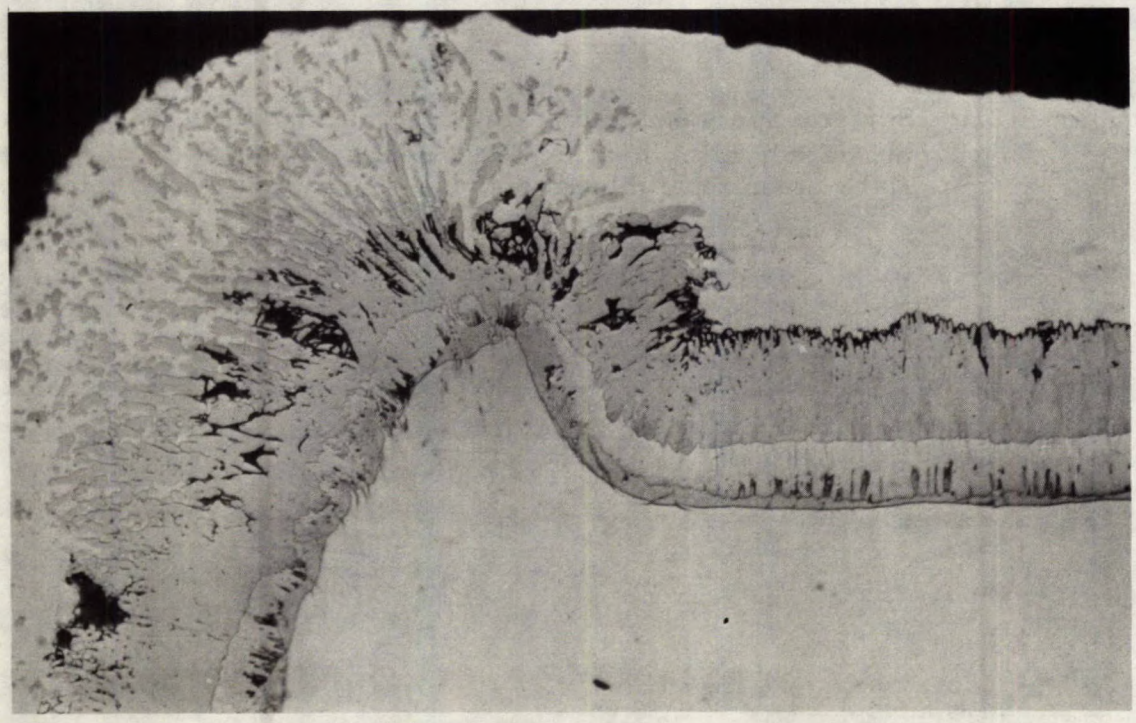

(b) 0.0015% Pb

Figure 14. Corner effects with lead-free and low-lead coatings (4-minute immersion) after heating for 8 hours at 300°C (570°F). X500

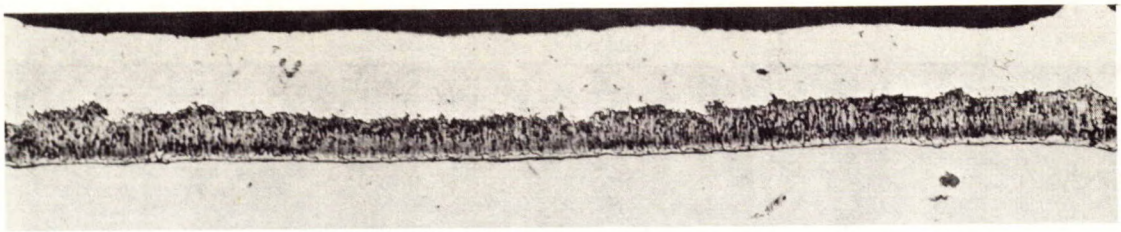

(a) As-galvanized (2 oz/sq ft)

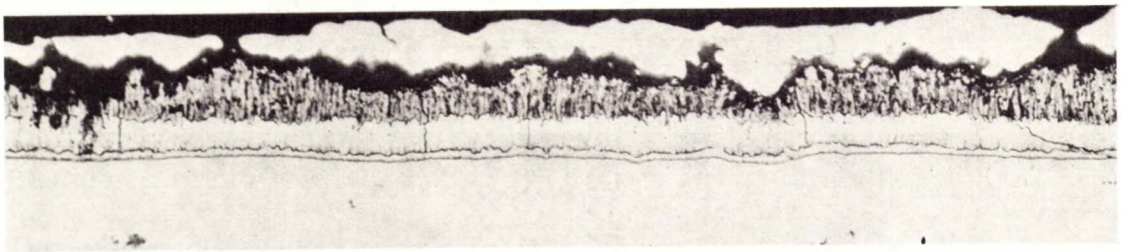

(b) 5 minutes

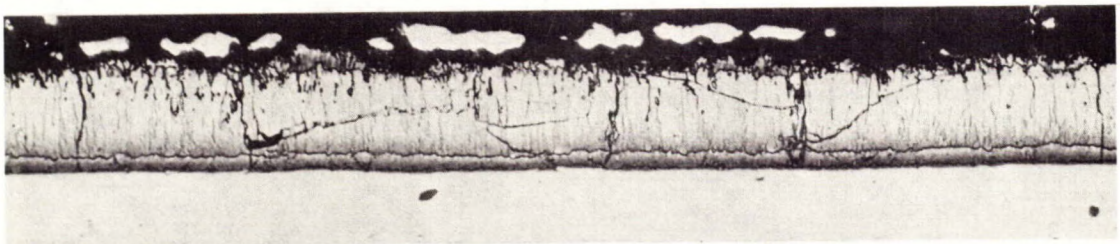

(c) 40 minutes

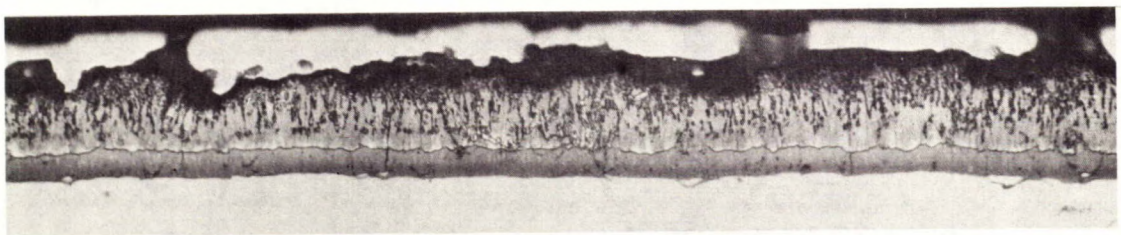

(d) 1 day

(e) 1 week

Figure 15. Commercial coating heated at 400°C (750°F). X500

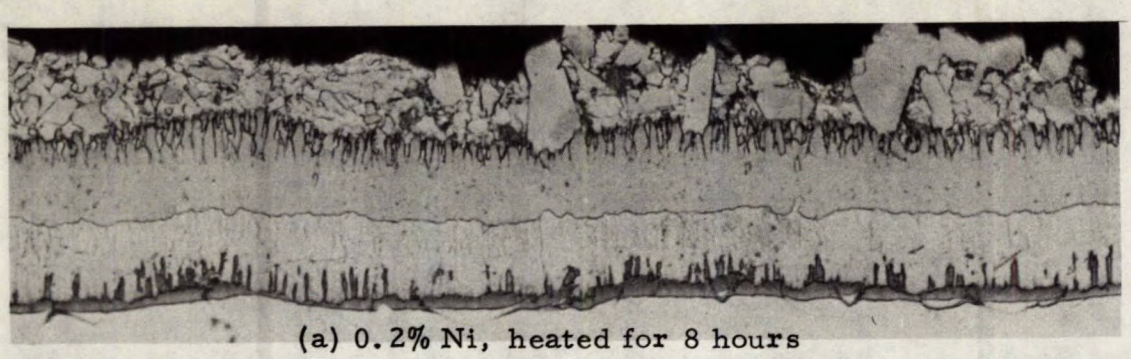

(a) 0.2% Ni, heated for 8 hours

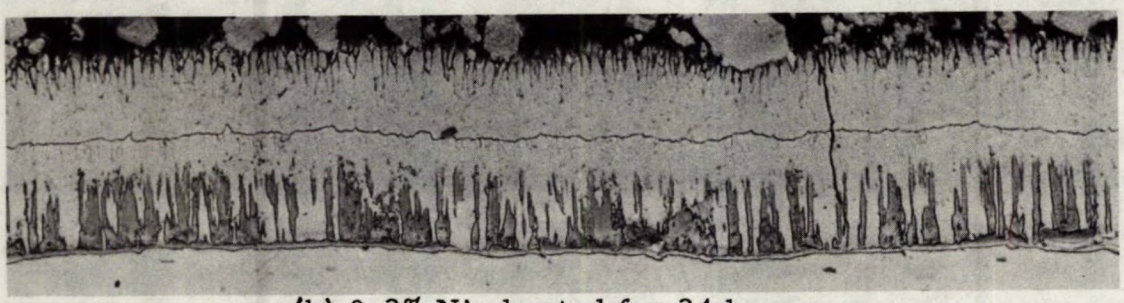

(b) 0.2% Ni, heated for 24 hours

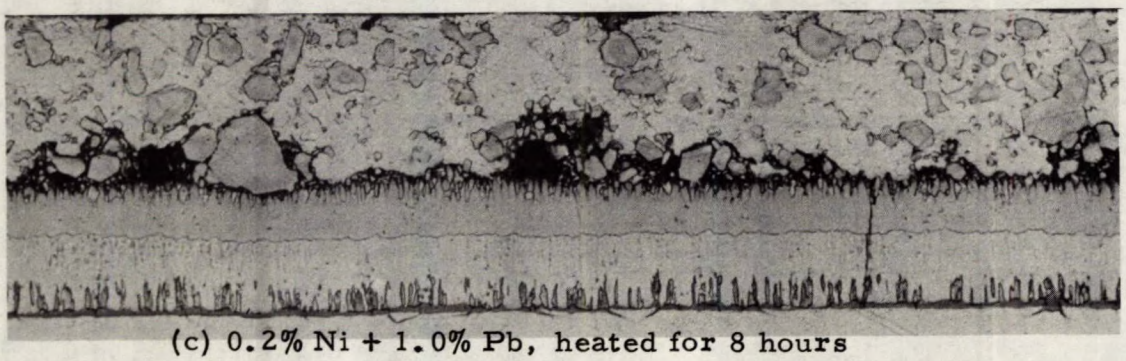

(c) 0.2% Ni + 1.0% Pb, heated for 8 hours

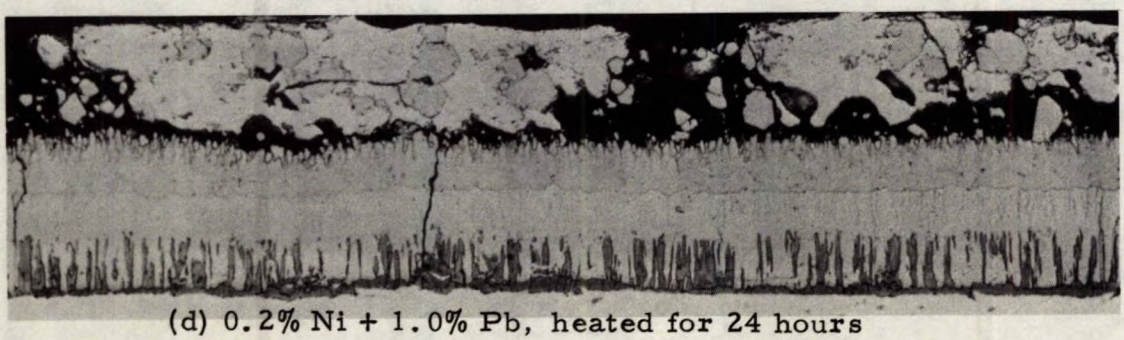

(d) 0.2% Ni + 1.0% Pb, heated for 24 hours

Figure 16. Nickel-containing coatings with and without lead (4-minute immersion), heated at 300°C (570°F). X500

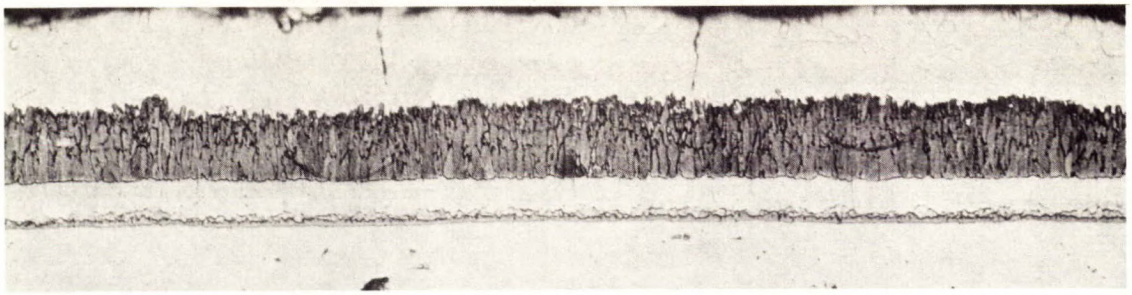

(a) As-galvanized (2.54 oz/sq ft)

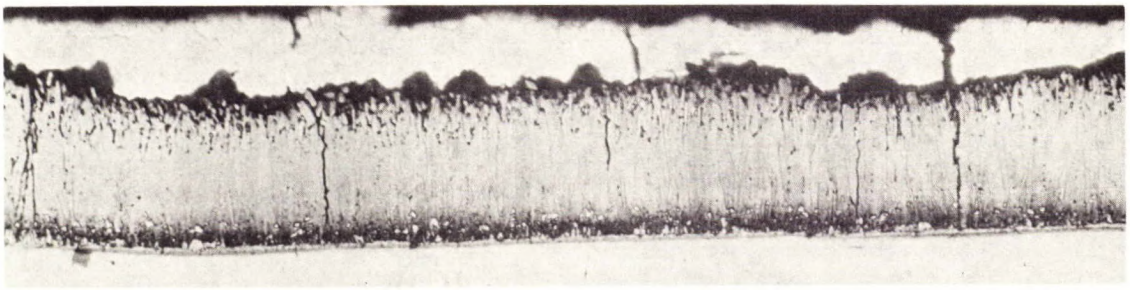

(b) 4 hours

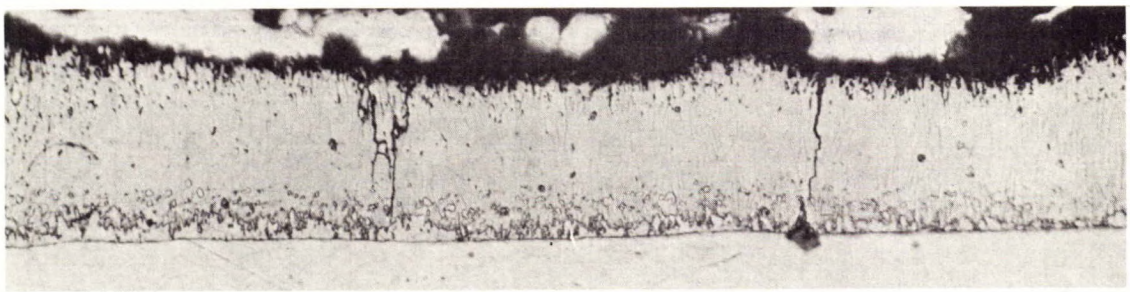

(c) 8 hours

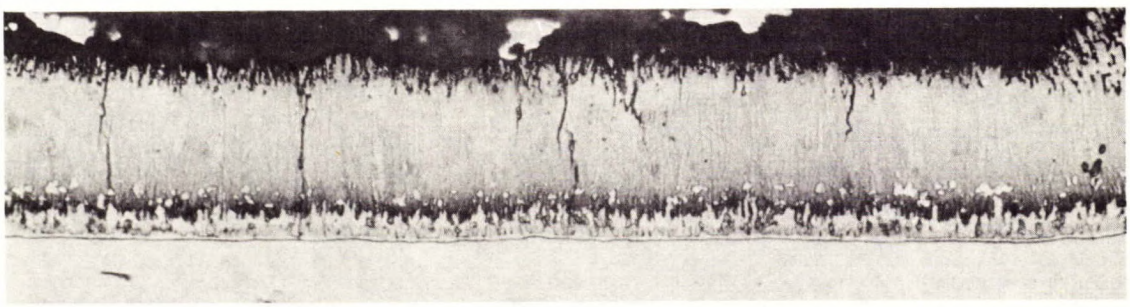

(d) 2 days

Figure 17. Tin-containing coatings (1.0% Sn, 4-minute-immersion), heated at 300°C (570°F). X500

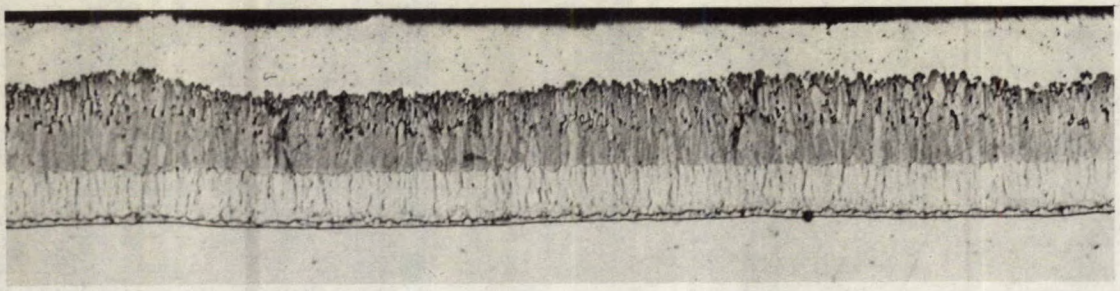

(a) 1.0% Bi, as galvanized (2.49 oz/sq ft)

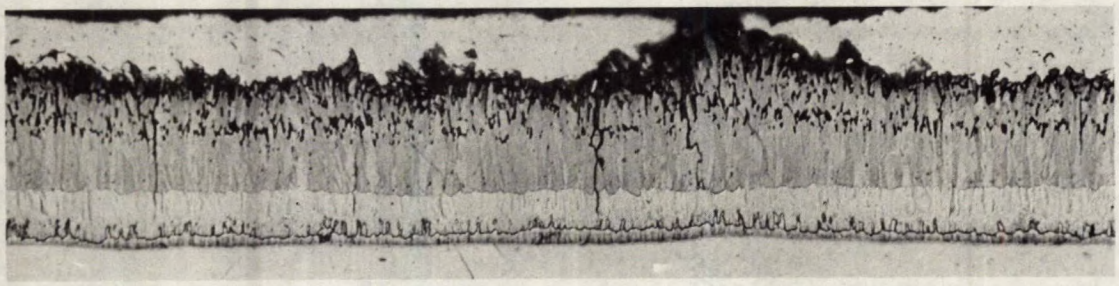

(b) 1.0% Bi, heated for 4 hours

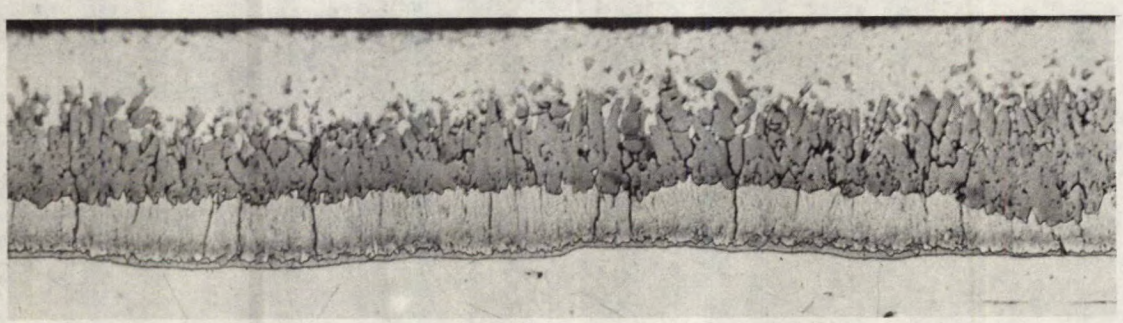

(c) 1.0% Bi + 1.0% Pb, as-galvanized (2.62 oz/sq ft)

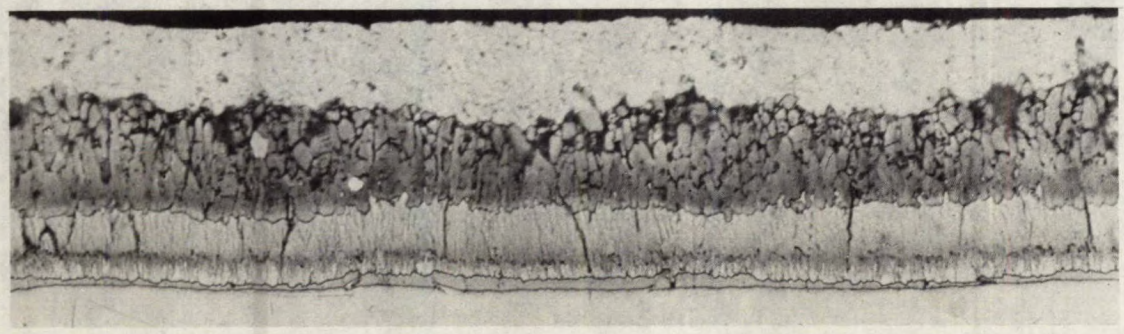

(d) 1.0% Bi + 1.0% Pb, heated for 8 hours

Figure 18. Bismuth-containing coatings with and without lead (4-minute immersion), heated at 300°C (570°F). X500

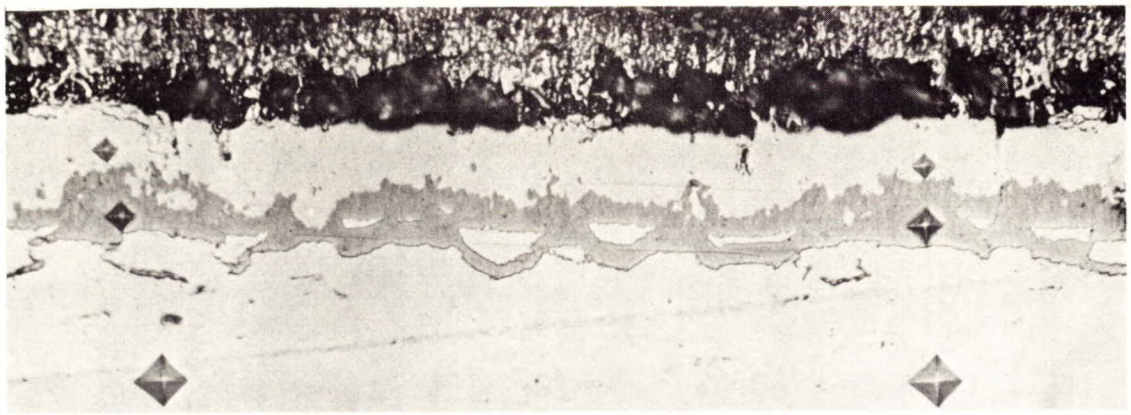

Figure 19. Microhardness variation in duplex-Γ layers (4-minute leaded coating heated for 2 weeks at 400°C (750°F). X500

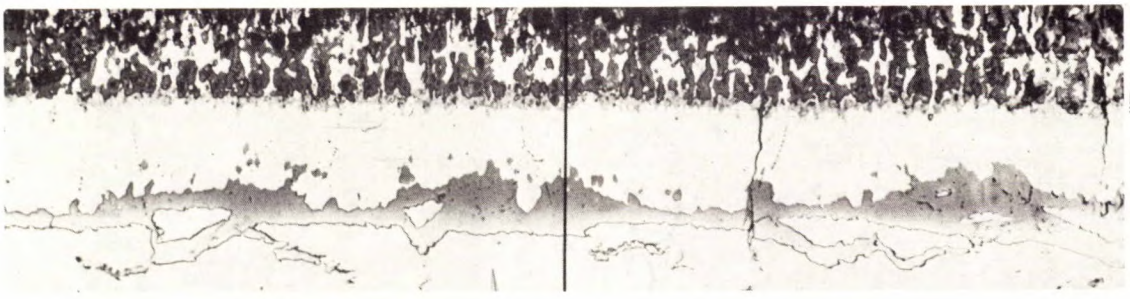

(a) Probe beam traverse on line indicated. X500

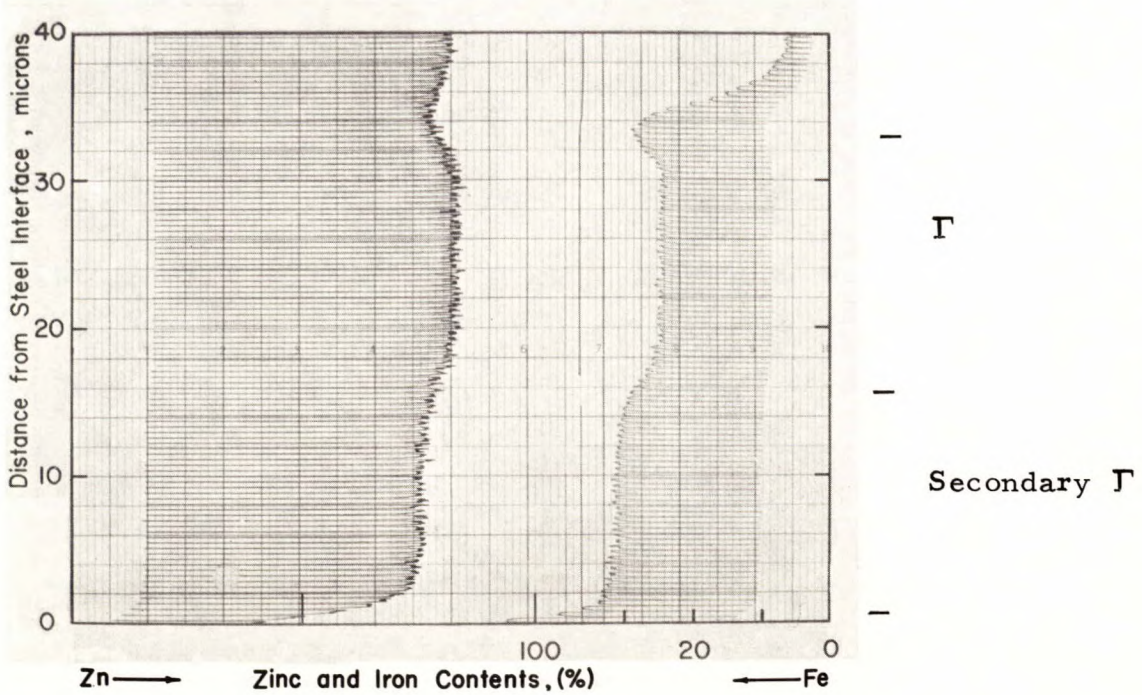

(a) Charted iron and zinc data for traverse in (a)

Figure 20. Electron-probe microanalysis of 4-minute leaded coating heated for 4 weeks at 400°C (750°F).